Sudden Cessation of Fluoxetine Before Alcohol Drinking Reinstatement Alters Microglial Morphology and TLR4/inflammatory Neuroadaptation in the Rat Brain

Jesús Aranda
IBIMA
María del Mar Fernández-Arjona
Universidad de Málaga: Universidad de Malaga
Francisco Alén
Universidad Complutense de Madrid
Patricia Rivera
IBIMA
Leticia Rubio
Universidad de Málaga Facultad de Medicina: Universidad de Malaga Facultad de Medicina
Inés Smith-Fernández
Universidad de Málaga Facultad de Medicina: Universidad de Malaga Facultad de Medicina
Francisco Javier Pavón
IBIMA
Antonia Serrano
IBIMA
Pedro J. Serrano-Castro
Hospital Regional Universitario de Málaga: Hospital Regional Universitario de Malaga
Fernando Rodríguez de Fonseca
IBIMA
Juan Suarez (juan.suarez@ibima.eu)
IBIMA. Hospital Regional Universitario de Malaga https://orcid.org/0000-0001-5254-9802

Research Article

Keywords: Alcohol, antidepressant, hippocampus, inflammation, microglia, fractal dimension.

Posted Date: May 18th, 2021

DOI: https://doi.org/10.21203/rs.3.rs-489428/v1

Version of Record: A version of this preprint was published at Brain Structure and Function on July 8th, 2021. See the published version at https://doi.org/10.1007/s00429-021-02321-9.

Abstract

Preclinical studies on the effects of abrupt cessation of selective serotonin reuptake inhibitors (SSRIs), a medication often prescribed in alcohol use disorder (AUD) patients with depression, results in alcohol consumption escalation after resuming drinking. However, a potential neuroinflammatory component on this escalation remains unexplored despite the immunomodulatory role of serotonin. Here, we utilized a rat model of 14-daily administration of the SSRI fluoxetine (10 mg/kg/day) along alcohol self-administration deprivation to study the effects of fluoxetine cessation on neuroinflammation after resuming alcohol drinking. Microglial morphology and inflammatory gene expression were analyzed in prelimbic cortex, striatum, basolateral amygdala and dorsal hippocampus. Results indicated that alcohol drinking reinstatement increased microglial IBA1 immunoreactivity and altered morphometric features of activated microglia (fractal dimension, lacunarity, density, roughness, and cell area, perimeter and circularity). Despite alcohol reinstatement, fluoxetine cessation modified microglial morphology in a brain region-specific manner, resulting in hyper-ramified (spatial complexity of branching), reactive (lower heterogeneity and circularity)-like microglia. We also found that microglial cell area correlated with changes in mRNA expression of chemokines (*Cx3cl1/fractalkine*, *Cxcl12/SDF1α*, *Ccl2/MCP1*), cytokines (*IL1β*, *IL6*, *IL10*) and the innate immune toll-like receptor 4 (*TLR4*) in dorsal hippocampus. Specifically, *TLR4* correlated with microglial spatial complexity assessed by fractal dimension in striatum, suggesting a role in process branching. These findings suggest that alcohol drinking reinstatement after fluoxetine treatment cessation disturbs microglial morphology and reactive phenotype associated with a TLR4/inflammatory response to alcohol in a brain region-specific manner, facts that might contribute to alcohol-induced damage through the promotion of escalation of alcohol drinking behavior.

Introduction

Alcohol is a psychoactive substance highly consumed in the general population worldwide [1]. Individuals having uncontrolled and problematic drinking (significant distress or harm) develop a complex clinical condition called alcohol use disorder (AUD) that can cause long-lasting changes in the brain that make patients vulnerable to relapse. AUD is characterized by its association with multiple comorbidities. One-third of AUD patients have a co-occurring mental health disorder, being anxiety and/or depression the most often diagnosed [2–4]. Likewise, one-fourth of people with mental health problems have a co-occurring substance use disorder, most commonly, AUD. This dual diagnosis is challenging since clinical outcomes of antidepressant treatment in co-morbid dual depression is poor and there is a need for analyzing antidepressant medications in a comprehensive, integrated approach. In this regard, pharmacological interventions using selective serotonin reuptake inhibitors (SSRIs), among others [5, 6], are able to reduce clinical symptoms of alcohol withdrawal including hyperlocomotion, anxiety and negative mood [7–10]. However, clinical relevance of SSRI pharmacotherapies to reduce alcohol harm is limited in AUD patients co-occurring liver and brain comorbidities such as liver steatosis, depression and/or cognitive impairment [11–13]. Indeed, SSRI treatments (i.e., fluoxetine and sertraline) have failed to achieve efficacy in reducing alcohol drinking and alcohol relapse [11, 14]. In addition, adherence to

antidepressant medication can fail if there is relapse to alcohol use, and the harms resulting of this discontinuation are far from being understood. Our previous studies have provided evidence that fluoxetine treatment cessation during alcohol deprivation facilitates alcohol seeking escalation during drinking reinstatement [15]. Recently, we have also suggested that dysregulation of glutamatergic receptor function and endocannabinoid signaling in the central amygdala likely underlies the contribution of SSRI treatment cessation in alcohol relapse [16].

The impact of alcohol on brain functions starts with neurochemical-specific adaptations that include critical modifications in the innate neuroimmune signaling [17–19], and changes in microglial function and phenotype involving morphology and neurochemical expression [20, 21]. Microglia are highly-sensitive cells that support innate immune response to alcohol through toll-like receptor 4 (TLR4) activation, a priming mechanism in ethanol-induced production of specific inflammatory cytokines (TNFα, IL1β) and chemokines (MCP1, eotaxin-1) in the brain [19, 22, 23]. Chronic overstimulation of microglia and the subsequence microglial production of cytokines including TNFα, IL1β, IL6 and TGFβ1 may contribute to neurotoxicity, neuronal cell death and brain atrophy associated with AUD [24–26]. Interestingly, periods of alcohol abstinence facilitate regenerative mechanisms of neuronal recovery such as increased neurogenesis in the dentate gyrus [27]. Evidence also suggests a role of TLR4 in neuropsychiatric diseases [28], and supports TLR4 signaling in stress-induced depression-like behaviors [29, 30], and ethanol-induced long-lasting cognitive dysfunctions [22] that likely confer a risk of dementia in AUD patients [31]. Regarding experimental models of AUD, reports coincide with clinical outcomes, providing evidence that long-term alcohol exposure reduces spatial memory, and increases the production of pro-inflammatory chemokines [32].

Recently, it has been hypothesized that fluoxetine might have potential neuroprotective effects through the induction of changes in both, microglial function and inflammatory responses involving TLR4/NF-kB signaling pathway [33–37]. Indeed, treatment with SSRIs decreases inflammatory cytokine elevations associated with major depression [38–41], but reduces microglial response to an inflammatory stimulus with lipopolysaccharide [42]. Despite the involvement of SSRIs in the modulation of neuroinflammation and alcohol seeking behavior, whether the abrupt cessation of fluoxetine treatment participates in the innate immune response to alcohol through changes in microglia morphology and inflammatory signals is presently unknown. The present study reveals that alcohol drinking reinstatement for 3 weeks after sudden cessation of fluoxetine treatment (10 mg/kg/day for 14 days) during alcohol self-administration deprivation modifies morphometric features of reactive microglia, and this effect is tightly correlated with specific changes in mRNA expression of anti- and pro-inflammatory cytokines (*TNFα*, *IL1β*, *IL*6, *IL4*, *IL10*, *TGFβ*, *BDNF*), chemokines (*Cx3cl1*, *Cxcl12*, *Ccl2*), and *TLR4* in a rat brain region-specific manner (prelimbic cortex, striatum, basolateral amygdala and dorsal hippocampus). Animals self-administering saccharine, receiving the same pattern of fluoxetine treatment, were used as control group.

Materials And Methods

Ethics statements

The protocols for animal care and use were approved by the Ethics and Research Committee at the University of Malaga (CEUMA registry no. 84-2015-A). All experimental procedures were performed in strict accordance with the Directive 2010/63/EU of the European Parliament and the EU Council (22 September 2010) and the Spanish regulation (RD 53/2013) on the protection of animals used for scientific purposes. We carried out the experiments in strict terms to minimize animal suffering and to reduce the number of animals used. Animal studies comply with the ARRIVE guidelines.

Animals

Thirty-eight male Wistar rats (Crl:WI, Charles Rivers, Barcelona, Spain), weighting 250 g and aging 10-12 weeks at the beginning of the experiments, were housed and allowed to acclimatize in standard conditions at 23 ± 1 °C room temperature, 40 ± 5% relative humidity and a 12-hours light-dark cycle with dawn/dusk effect. Tap water and standard rodent chow (Prolab RMH 2500, 2.9 kcal/g) were available *ad libitum*. The animals had 2 weeks for the adjustment of the environmental conditions, before the implementation of the self-administration training protocol.

Drugs

Alcohol solution (10% alcohol w/v solution) was prepared daily from 99% ethanol. Solution of fluoxetine HCl (Prozac®, Eli Lilly, Alcobendas, Spain) was also prepared daily by dissolving in 0.9% saline, and were injected intraperitoneally (i.p.) at a concentration of 10 mg/kg in a volume of 2 mL/kg body weight as previously described [15,16].

Operant alcohol self-administration

A total of 26 animals were trained according to a paradigm of operant ethanol self-administration as previously described [5,16]. We used an alcohol relapse model based on the alcohol deprivation effect, which consist to have excellent face and predictive validity in relation to alcohol consumption supported by previous studies [5,15,16,43]. Briefly, after lever-press training habituation by using a 0.2% saccharine facing procedure [15] in operant cages set with liquid dispenser (LE850W, Panlab, Barcelona, Spain), all animals were then introduced in alcohol operant sessions consisted of 30 min/day over a 5 day/week (Monday to Friday) following a proportional sequence of saccharine/ethanol (0.16/2 for 3 sessions; 0.12/4 for 3 sessions; 0.08/6 for 4 sessions; 0.04/8 for 4 sessions; 0.02/10 for 4 sessions; and finally 10% ethanol for the remaining sessions) on a fixed-ratio 1 schedule until steady levels of alcohol self-administration were achieved (baseline, 30 presses with less than 15% variation in 2 consecutive days). Pressing the active lever resulted in the delivery of 0.1 mL of the ethanol solution (time-out of 2.5 seconds). After that alcohol self-administration was withdrawn (abstinence) and the 26 animals were randomly assigned to be daily treated with fluoxetine (10 mg/kg) or vehicle (saline) for 14 days (n = 13/group). Then, 24 hours after treatment was ceased, alcohol self-administration sessions of 30 min/day were re-introduced (reinstatement) for 3 consecutive weeks (**Fig. 1A**). Twelve additional rats were trained for saccharine self-administration following the same schedule and operant sessions as those followed by the ethanol-exposed rats. In the same way, rats were randomly treated with fluoxetine

(10 mg/kg) or vehicle (saline) for 14 days (*n* = 6/group). Finally, saccharine self-administration sessions were re-introduced for 3 weeks.

Sample Collection

One hour after the last alcohol/saccharine self-administration session, all animals were anaesthetized with sodium pentobarbital (50 mg/kg, i.p.). Some animals (*n* = 6/group) were perfused transcardially with 4% formaldehyde in 0.1 M phosphate buffer (PB). Whole brains were extracted and processed for -80 °C cryopreservation with 30% sucrose in PB. The brains were then cut into 30-µm-thick coronal sections by using a freezing microtome (Leica SM2000R). Sections were stored at 4 °C in PB with 0.002% (*w/v*) sodium azide until they were used for immunohistochemical analysis. Remaining animals (*n* = 7/group) were sacrificed by decapitation, brains were collected, and the prelimbic cortex (PrL, also called medial prefrontal cortex), striatum (Str), basolateral amygdala (BLA) and dorsal hippocampus were dissected and stored at -80 °C until they were used for mRNA expression analysis by RT-qPCR technique.

Immunohistochemistry

Free-floating coronal sections were selected from 5.16 to 2.52 mm, 2.28 to -0.12 mm, -2.04 to -3.60 mm and -2.04 to -4.68 mm of Bregma levels [44], corresponding to PrL, Str, BLA and dorsal hippocampus, respectively (**Fig. 1C**). A minimum of 8 sections per brain region were selected from one of the 6 parallel series obtained from each rat brain of the 4 experimental groups (n = 6/group). Sections were immunostained simultaneously using a four-well plate (aprox. 48 sections/well). Sections were incubated overnight at 4 °C in the following diluted primary antibody: polyclonal rabbit anti-IBA-1 (1:1000, cat. no. 019-19741, Wako, Neuss, Germany. RRID: AB_839504). After antibody incubation, the sections were washed and incubated in biotinylated donkey anti-rabbit IgG (1:500, cat. no. RPN1004, GE Healthcare, Barcelona, Spain. RRID: AB_1062582) at room temperature for 2 h. Then, the sections were incubated in ExtrAvidin®-Peroxidase (1:2000, cat. no. E2886, Sigma-Aldrich-Merck, Darmstadt, Germany. RRID: AB_2620165) in darkness at room temperature for 1 h. Finally, immunolabeling was revealed with 0.05% diaminobenzidine (DAB, Sigma-Aldrich), 0.05% nickel ammonium sulfate (Ni) and 0.03% H_2O_2 in PB-saline for at least 10 min.

Stereological cell quantification

Representative counting frames were obtained using a standard optical microscope equipped with the 40x objective (Nikon Instruments Europe B.V., Amstelveen, The Netherlands) and coupled to the NIS-Elements Imaging Software 3.00 (Nikon). The brain regions of interest for this study were: PrL, Str, BLA, and the hippocampal areas CA1 and CA3, and the dentate gyrus. A minimum of 8 coronal sections per brain region was analyzed, which resulted in one of every six equidistant sections (one representative section for each 180 µm) according to the rostro-caudal extent. Estimations of the number of IBA-1-immunoreactive (+) cells per area (mm^2) in both hemispheres were manually counted according to stereological methods and calculated based on the following formula (Rivera et al., 2018):

$$Na = \Sigma(Q-)/\Sigma(astr),$$

where ΣQ− is the total number of positive (+) cells counted per animal, and a_{str} is the area (mm^2) of the structure analyzed. Cell number quantification was expressed as the average number of IBA-1+ cells per area (mm^2) for each experimental group. For densitometric analysis, quantification of IBA1 immunoreactivity is determined using ImageJ software (NIH, USA) and expressed as arbitrary units of average intensity of the image field that corresponds to representative areas of the brain regions.

Morphometric analysis

Image acquisition was carried out with the aim of morphometric analysis of microglial cells. For this purpose, digital color images of PrL, Str, BLA and CA1 sections immunolabeled with IBA-1 antibody and DAB-Ni were obtained using an Olympus VS120 microscope. The UPLSAPO 60xO oil immersion objective was used to capture high-resolution images (pixel size side = 115 nm) of the selected areas. A multi-plane virtual-Z mode allowed to capture 20 images (1 µm thick) in 20 µm depth of the tissue section, which were later combined to obtain a single high-quality image including detailed magnification of ramified processes of the cells. Each obtained image was a TIFF file of 96 ppi and contained at least 30 cells. These images were cropped to delimit single cells according to the following criteria: (i-a) random selection in prefrontal cortex areas corresponding to the prelimbic cortex (PrL); (i-b) random selection starting from the area nearest to the lateral ventricle (LV) towards the brain parenchyma up to a depth of about 100 µm into the dorsal part of the striatum (Str); (i-c) random selection in the basolateral amygdala (BLA); and (i-d) random selection throughout the striati radiatum (SR) and lacunosum-moleculare (SL-M) of the hippocampal CA1 region; (ii) no overlapping with neighboring cells; and (iii) complete nucleus and branches (at least apparently). Selection was blinded to alcohol and treatment. Fifty cells randomly selected from 6 animals per experimental group and brain region were analyzed. A total of 800 images was evaluated. Each single cell image was processed in a systematic way using FIJI free software, an application from the ImageJ software. After the image processing of each single cell, we obtained a “filled image” and its counterpart “outlined shape” as previously described [21,45]. These filled and outlined cell images were subsequently used for morphometric analysis. Morphological features of microglial cells were quantified with the free software FracLac for ImageJ ([46]; FracLac for ImageJ; available at the ImageJ website, NIH). The following 15 parameters were measured as previously described [45]: (1) *fractal dimension* (D); (2) *lacunarity* (□); (3) *cell area* (CA, μm^2); (4) *cell perimeter* (CP, µm); (5) *cell circularity* [ ]; (6) *convex hull area* (CHA, μm^2); (7) *density* (ρ, CA/CHA); (8) *convex hull perimeter* (CHP, µm); (9) *roughness* (CP/CHP); (10) *convex hull circularity* [ ]; (11) *convex hull span ratio* (CHSR, M/m); (12) *diameter of the bounding circle* (BCD, µm); (13) *maximum span across the convex hull* (MSACH, µm); (14) *the ratio maximum/minimum convex hull radii* (RCHR, R/r); and (15) *the mean radius* (MR, µm).

RNA isolation and RT-qPCR analysis

RT-qPCR (Taqman, Applied Biosystem, Carlbad, CA, USA) was performed in a CFX96TM Real-Time PCR Detection System (Bio-Rad, Hercules, CA, USA), using specific sets of primer probes (**Table 1**) and the FAM dye label format for the Taqman® Gene Expression Assays (ThermoFisher), as described previously (Rivera et al., 2018). Briefly, Prl, Str, BLA and dorsal hippocampal samples were homogenized on ice and RNA was extracted following Trizol® method according to the manufacture's instruction (Gibco BRL Life Technologies, Baltimore, MD, USA). RNA was isolated, and reverse transcript reaction (RT, 1 µg of RNA) and quantitative real-time reverse transcription polymerase chain reaction (qPCR) were performed. Melting curve analysis was obtained to ensure that only a single product was amplified. Ct values from mRNA expression of inflammatory factors were normalized in relation to those Ct values from *Gapdh* mRNA expression.

Statistical Analysis

Comparisons of data were carried out by using GraphPad Prism 6.0 (GraphPad Software, San Diego, CA, USA). The data on IBA-1 immunoreactivity, IBA-1+ cell number per area (mm^2), morphometric parameters of microglia, and relative mRNA expression of inflammatory factors were represented as means ± Standard Error of the Mean (SEM). The n indicates the number of animals (n = 6-7) or cells recorded (n = 50) per experimental group. Kolmogorov-Smirnov normality test was used to verify Gaussian distribution. Statistical significance for IBA-1 immunohistochemistry and microglial morphology were determined by repeated/two-way ANOVA with time (weeks), drinking (saccharine *vs*. ethanol) and treatment (vehicle *vs*. fluoxetine) as main factors, followed by Tukey's *post hoc* tests for multiple comparison where appropriate. Statistical significance for mRNA expression was determined by unpaired Student's *t*-test. To analyze whether fluoxetine treatment cessation induced changes in the association between parameters, correlation model analysis was performed and *Rho* values (goodness-of-fit) calculated. A *P* value less than 0.05 indicates statistical significance.

Results

Fluoxetine treatment cessation increases ethanol self-administration during reinstatement

As expected, a significant increase in weekly ethanol self-administration during the re-exposure period (reinstatement) was detected in the rats that were previously treated with fluoxetine during the ethanol deprivation period (**Fig. 1B**). Repeated measures ANOVA indicated an overall treatment effect on ethanol self-administration for 3 weeks ($F_{1,72}$=26.66, p<0.0001), with fluoxetine-treated rats having higher consumption of ethanol during reinstatement (*post hoc* comparisons: *p<0.05 *vs*. ethanol-exposed rats treated with vehicle). Interaction between time and treatment was found when baseline period was introduced in the statistical analysis ($F_{3,96}$=3.56, p<0.02), suggesting that fluoxetine treatment cessation modified ethanol self-administration during reinstatement compared to ethanol self-administration baseline.

Ethanol drinking reinstatement increases IBA-1 immunoreactivity in the brain

To analyze the effects of the abrupt cessation of fluoxetine treatment during ethanol abstinence and ethanol drinking reinstatement on the presence of microglia in the rat brain, we quantified the IBA-1+ cell number and IBA-1 immunoreactivity (intensity) in the PrL, Str, BLA, and the hippocampal areas CA1 and CA3, and the dentate gyrus.

Alcohol, but not saccharine drinking induced significant overall effects on the IBA-1 immunoreactivity, but not IBA-1+ cell number, in the PrL ($F_{1,20}$=12.13, p=0.0027), Str ($F_{1,20}$=29.88, p<0.0001) and BLA ($F_{1,20}$=46.08, p<0.0001), showing a higher intensity in both ethanol-exposed rats (*post hoc* comparisons: **/***p<0.01/0.001 *vs*. saccharine-exposed rats) and ethanol-exposed rats treated with fluoxetine (*post hoc* comparisons: $^{\$\$\$}p$<0.001 *vs*. saccharine-exposed rats treated with fluoxetine, **Figs. 2A-I**). Treatment overall effect and interaction between drinking and treatment were not detected in the three brain regions.

Drinking induced a significant overall effect on IBA-1+ cell number in the dorsal hippocampus ($F_{1,20}$=15.03, p=0.001), showing a specific increase in the dentate gyrus (overall effect: $F_{1,20}$=154.4, p<0.0001), but not CA3 and CA1 areas, of both ethanol-exposed rats (*post hoc* comparisons: ***p<0.001 *vs*. saccharine-exposed rats) and ethanol-exposed rats treated with fluoxetine (*post hoc* comparisons: $^{\$\$\$}p$<0.001 *vs*. saccharine-exposed rats treated with fluoxetine, **Figs. 3A-C**). Drinking also resulted in an overall effect on IBA-1 immunoreactivity in the dorsal hippocampus ($F_{1,20}$=31.36, p<0.0001), including dentate gyrus ($F_{1,20}$=21.41, p<0.001), CA3 ($F_{1,20}$=22.15, p<0.001) and CA1 ($F_{1,20}$=32.67, p<0.0001). As a consequence, ethanol increased IBA-1 immunoreactivity in these hippocampal regions of both ethanol-exposed rats (*post hoc* comparisons: **/***p<0.01/0.001 *vs*. saccharine-exposed rats) and ethanol-exposed rats treated with fluoxetine (*post hoc* comparisons: $^{\$/\$\$}p$<0.05/0.01 *vs*. saccharine-exposed rats treated with fluoxetine, **Figs. 3D-F**). Treatment overall effect and interaction between drinking and treatment were not detected in dorsal hippocampus. Representative images of the immunohistochemical expression of IBA-1 and apparent density of IBA-1+ cells are shown in **Figs. 3G-I**.

Fluoxetine treatment cessation before ethanol drinking reinstatement modifies microglial morphology in a brain region-specific manner

We assessed whether increases in IBA-1 immunoreactivity induced by ethanol are associated with changes in morphometric parameters of microglial cells expressing IBA-1 in the PrL, Str, BLA and the hippocampal CA1 region. We also evaluated whether fluoxetine treatment cessation modifies the putative ethanol effect on microglial morphology.

Analysis of interaction and main overall effects of drinking and treatment

Significant overall effects of drinking (saccharine *vs*. ethanol) on fractal dimension (spatial complexity), lacunarity (heterogeneity), roughness (process surface and branching), and cell area, perimeter and circularity were detected in the microglia of the PrL (**Table 2**). We also observed significant overall effects of drinking on most morphometric parameters, excepting lacunarity, convex hull span ratio (CHSR) and the maximum/minimum convex hull radii (RCHR), in the microglia of the Str. Significant effects of

drinking on lacunarity and density (process shortening/thickening) were only observed in the microglia of the BLA. Finally, significant overall effects of drinking on most morphometric parameters, excepting lacunarity, density, cell circularity, convex hull circularity (CHC), bounding circle diameter (BCD) and maximum span across the convex hull (MSACH), were observed in the microglia of the hippocampal CA1 region (**Table 2**).

Significant overall effects of treatment (vehicle *vs*. fluoxetine) on BCD, MSACH, and the mean radius (MR) were detected in the microglia of the PrL, and no treatment effect on the morphometric parameters in the microglia of the BLA was found (**Table 2**). Prominently, we found significant overall effects of treatment on fractal dimension, roughness, cell perimeter and circularity, and convex hull area and perimeter in the microglia of the Str. Significant overall treatment effects on fractal dimension, cell circularity, convex hull area, perimeter and circularity, density, BCD, MSACH, and MR were also found in the microglia of the hippocampal CA1 region (**Table 2**).

Interaction between factors (drinking *vs*. treatment) was only observed in roughness in the microglia of the PrL, suggesting a specific increase in process surface and branching in ethanol-exposed rats that were previously treated with fluoxetine. Regarding the striatum, interaction was mainly detected in microglial cell circularity (**Table 2**), suggesting that fluoxetine decreases the proportion between microglial cell area and perimeter in a drinking-dependent manner. In the microglia of CA1 region, interaction was found in fractal dimension, lacunarity and density, with fluoxetine decreasing spatial complexity and increasing heterogeneity and process length/thinning in a drinking-dependent manner. Interaction was not observed when morphometric parameters of microglia were analyzed in BLA (**Table 2**).

Simple effect analysis of fractal dimension, lacunarity, and cell area, perimeter and circularity

Following two-way ANOVA of main factors, Tukey's *post hoc* for multiple comparisons were conducted when appropriate. Ethanol increased fractal dimension (spatial comlexity) in the Str of vehicle-treated rats (**p*<0.05, **Fig. 4B**), as well as fractal dimension in the PrL, Str, BLA and CA1 of rats treated with fluoxetine ($^{\$/\$\$}$*p*<0.05/0.01, **Figs. 4A-D**). Fractal dimension is increased in the Str and decreased in the CA1 of saccharine-exposed rats that were previously treated with fluoxetine (**p*<0.05, **Figs. 4B, 4D**). Ethanol decreased lacunarity (heterogeneity) in the CA1 of vehicle-treated rats (**p*<0.05, **Fig. 4H**), as well as lacunarity in the PrL and CA1 of fluoxetine-treated rats ($^{\$\$}$*p*<0.01, **Figs. 4E, 4H**). Fluoxetine increased lacunarity in the PrL and CA1 of saccharine-exposed rats (*/****p*<0.05/0.001, **Figs. 4E, 4H**). Microglial cell area (process branching and/or soma enlargement) was increased by ethanol in the Str and CA1 of vehicle-treated rats (**/****p*<0.01/0.001, **Figs. 4J, 4L**), as well as in the PrL, Str, BLA and CA1 of fluoxetine-treated rats ($^{\$/}$

/

$^{\$}$*p*<0.05/0.01/0.001, **Figs. 4I-L**). Microglial cell area was decreased in the PrL and increased in the Str of saccharine-exposed rats that were previously treated with fluoxetine (**p*<0.05, **Figs. 4I, 4J**). Interestingly,

fluoxetine increased microglial cell area in the CA1 of ethanol-exposed rats ($^{\#}p$<0.05, **Fig. 4L**). Ethanol increased microglial cell perimeter in the Str and CA1 of vehicle-treated rats ($^{*/**}p$<0.05/0.01, **Figs. 4N, 4P**), as well as cell perimeter in the PrL and CA1 of fluoxetine-treated rats ($^{\$/\$\$\$}p$<0.05/0.001, **Figs. 4M, 4P**). Ethanol decreased microglial cell circularity in the Str of vehicle-treated rats (***p<0.001, **Fig. 4R**), as well as cell circularity in the PrL of fluoxetine-treated rats ($^{\$\$}p$<0.01, **Fig. 4Q**). Fluoxetine also decreased cell circularity in the Str and CA1 of saccharine-exposed rats (**p<0.01, **Figs. 4R, 4T**). Interestingly, fluoxetine specifically decreased cell circularity in the CA1 of ethanol-exposed rats ($^{\#}p$<0.05, **Fig. 4T**).

Simple effect analysis of density, roughness, and convex hull area, perimeter and circularity

Following two-way ANOVA of main factors, Tukey's *post hoc* for multiple comparisons were conducted when appropriate. Ethanol increased convex hull (CH) area in the Str and CA1 of vehicle-treated rats (**p<0.01, **Figs. 5B, 5D**), as well as CH area in the PrL and CA1 of fluoxetine-treated rats ($^{\$}p$<0.05, **Figs. 4A, 5D**). Fluoxetine decreased CH area in the PrL and BLA, but increased CH area in the Str and CA1 of saccharine-exposed rats ($^{*/**}p$<0.05/0.01, **Figs. 5A-D**). Ethanol increased density in the BLA of vehicle-treated rats (**p<0.01, **Fig. 5G**), as well as density in the Str and CA1 of fluoxetine-treated rats ($^{\$/\$\$}p$<0.05/0.01, **Figs. 5F, 5H**). In contrast, fluoxetine specifically decreased density in the CA1 of saccharine-exposed rats (***p<0.001, **Fig. 5H**). Ethanol increased CH perimeter in the Str and CA1 of vehicle-treated rats ($^{*/**}p$<0.05/0.01, **Figs. 5J, 5L**), as well as CH perimeter in the PrL of fluoxetine-treated rats ($^{\$}p$<0.05, **Fig. 5I**). Similar to CH area, fluoxetine decreased CH perimeter in the PrL and BLA, but increased CH perimeter in the Str and CA1 of saccharine-exposed rats ($^{*/**}p$<0.05/0.01, **Figs. 5I-L**). Ethanol increased roughness in the Str and CA1 of vehicle-treated rats (*/**p<0.05/0.01, **Figs. 5N, 5P**), as well as roughness in the PrL, BLA and CA1 of fluoxetine-treated rats ($^{\$/}$

/

$^{\$}p$<0.05/0.01/0.001, **Fig. 5M**, **5O, 5P**). Fluoxetine specifically increased roughness in the Str of saccharine-exposed rats (*p<0.05, **Fig. 5N**). Fluoxetine also increased cell circularity in the BLA and CA1 of ethanol-treated rats ($^{\#/\#\#\#}p$<0.05/0.001, **Figs. 5S, 5T**), as well as cell circularity in the CA1 of the saccharine-treated rats (***p<0.001, **Fig. 5T**).

Simple effect analysis of convex hull span ratio, bounding circle diameter, maximum span across the convex hull, the ratio maximum/minimum convex hull radii, and the mean radius

Following two-way ANOVA of main factors, Tukey's *post hoc* for multiple comparisons were conducted when appropriate. Ethanol specifically decreased CH span ratio in the CA1 of both vehicle- and fluoxetine-treated rats ($^{***/\$\$\$}p$<0.001, **Fig. 6D**). Ethanol increased bounding circle diameter (BCD) and maximum span across the convex hull (MSACH) in the Str of vehicle-treated rats (*/**p<0.05/0.01, **Figs. 6F, 6J**). In contrast, fluoxetine decreased BCD and MSACH in the PrL, but increased these parameters in the Str and CA1 of saccharine-exposed rats (*p<0.05, **Figs. 6E, 6F, 6H, 6I, 6L**). Similar to CH span ratio, ethanol decreased the ratio maximum/minimum CH radii (RCHR) in the CA1 of both vehicle- and fluoxetine-

treated rats (***/$$$$p<0.001/0.01, **Fig. 6P**), as well as RCHR in the BLA of fluoxetine-treated rats ($p<0.05, **Fig. 6O**). Ethanol increased the mean radius (MR) in the Str and CA1 of vehicle-treated rats (*/***p<0.05/0.001, **Figs. 6R, 6T**), as well as MR in the PrL of fluoxetine-treated rats ($p<0.05, **Fig. 6Q**). In contrast, fluoxetine decreased MR in the PrL, but increased MR in the Str and CA1 of saccharine-exposed rats (*p<0.05, **Figs. 6Q, 6R, 6T**).

Microglia morphology correlates with fluoxetine-induced changes in inflammatory factors and TLR4 in a brain region-specific manner

Since alcohol induced specific activation of microglia, as measured by IBA1 immunoreactivity, we evaluated whether fluoxetine treatment cessation modifies mRNA expression of inflammatory factors (cytokines and chemokines) and *TLR4* in the PrL, Str, BLA and the hippocampal CA1 region of those rats with alcohol drinking reinstatement. We also assessed whether specific morphometric features of microglia are tightly associated with changes in inflammatory factors induced by fluoxetine.

Fluoxetine reduced mRNA expression of the pro-inflammatory chemokine *Cx3cl1* (*fractalkine*), and increased mRNA expression of the inflammatory cytokines *IL1b* and *IL10* in the PrL of ethanol-exposed rats (*p<0.05, **Fig. 7A**). Fluoxetine only increased mRNA expression of *TLR4* in the Str of ethanol-exposed rats (*p<0.05, **Fig. 7B**). Fluoxetine also reduced mRNA expression of the chemokine *Cx3cl1*, and increased mRNA expression of the anti-inflammatory cytokines *IL4* in the BLA of ethanol-exposed rats (*p<0.05, **Fig. 7C**). Fluoxetine also reduced mRNA expression of the chemokine *Cx3cl1*, and increased mRNA expression of most of the remaining chemokines (*Cxcl12*, *Ccl2*) and cytokines (*IL1β*, *IL6*, *IL10*) analyzed, as well as *BDNF* and *TLR4*, in the dorsal hippocampus of ethanol-exposed rats (*p<0.05, **Fig. 7D**).

When we analyzed whether morphometric parameters of microglia correlated with these changes of inflammatory factors induced by fluoxetine, we specifically detected that fractal dimension (microglial spatial complexity) positively correlated with mRNA expression of *IL10* (*R*= 0.67, *p*<0.009), and negatively correlated with mRNA expression of *Cx3cl1* (*R*= -0.53, *p*<0.05) in the PrL (**Fig. 7E**). We also found that fluoxetine-induced increase in *TLR4* expression specifically correlated with higher values of fractal dimension in the Str (*R*= 0.64, *p*<0.05, **Fig. 7F**). In the BLA (**Fig. 7G**), fractal dimension correlated with higher mRNA expression of *IL4* (*R*= 0.85, *p*=0.0001), and lower mRNA expression of *Cx3cl1* (*R*= -0.60, *p*<0.03) and *Ccl2* (R= -0.65, p<0.02). Finally, in the dorsal hippocampus (**Fig. 7H**), microglial cell area (process branching and/or soma enlargement) positively correlated with fluoxetine-induced increases in mRNA expression of most factors analyzed (*Cxcl2*, *Ccl2*, *IL1β*, *IL6*, *IL10*, *BDNF*, *TLR4*: *R*> 0.55, *p*<0.04), and negatively correlated with fluoxetine-induced decreases in mRNA expression of *Cx3cl1* (*R*= -0.66, *p*<0.01).

Discussion

Alcohol use disorder (AUD) results in neuroimmune consequences that contribute to depression [47,48]. One of the key elements of this pro-inflammatory actions of alcohol is the direct activation of TLR4

receptors in the brain [49]. Although the use of SSRI-antidepressants in the context of AUD when depression is present is controversial [7], its putative anti-inflammatory pharmacotherapeutic properties have promoted its use in AUD, despite of the incongruences described on its anti-inflammatory action [35,41].

In the present study, we evaluated the inflammatory effects of alcohol drinking reinstatement (3 weeks) on microglial morphology and reactive phenotype after an experimental condition characterized by alcohol intake escalation derived from the abrupt cessation of fluoxetine treatment (10 mg/kg/day) given along a period of alcohol self-administration deprivation (14 days). Animals self-administering saccharine, receiving the same pattern of fluoxetine treatment, were used as control group. We observed that alcohol drinking reinstatement increases brain immunoreactivity for IBA-1 in all brain regions studied. IBA-1 is a protein that participates in the cytoskeleton of microglia [50] and it is induced by inflammatory events, serving as an immunohistochemical marker of reactive microglia. Increases in IBA-1 immunohistochemical expression induced by ethanol are associated with changes in microglial morphology that likely depicts an activated state. Interestingly, differences in main morphometric parameters of microglia (fractal dimension, lacunarity, density, roughness, and cell area, perimeter and circularity) were observed in a brain region-specific manner (**Fig. 8**). Particularly, among the brain regions analyzed, the striatum and hippocampal CA1 area showed prominent alterations in microglial morphology (higher spatial complexity, branching and perimeter surface), supporting a ramified state of the microglia induced by alcohol drinking reinstatement. Despite the lack of effect of fluoxetine treatment cessation on IBA-1 immunoreactivity (a lack of effects also observed in saccharine-drinking animals), subtle changes in highly-sensitive parameters of microglial morphology (fractal dimension, lacunarity, cell area and circularity, density, roughness) were detected after fluoxetine treatment cessation, resulting in a hyper-ramified, reactive-like microglia in the striatum and hippocampal CA1 area. Specifically, CA1 microglia showed an increase in cell area (process branching and/or soma enlargement) and a decrease in cell circularity (proportional index between cell area and perimeter). These morphological changes might be linked to the escalation of alcohol intake found after fluoxetine cessation [15,16], since synapses remodeling underlying enhanced alcohol seeking/consumption behaviors needs activated microglia to readjust motivational and cognitive circuits regulating alcohol intake. This attractive hypothesis needs to be confirmed with further research.

Studies investigating the effects of alcohol exposure on microglial activation in different animal models (chronic, intermittent and binge consumption over several days, weeks and months in adult and neonatal rodents) describe increases in gene or protein expression of the microglial marker IBA-1 in the hippocampus and cerebral cortex [32,51-54]. In agreement with these results, we also observed increases in the immunohistochemical expression of IBA-1 in PrL (also known as medial prefrontal cortex), striatum, basolateral amygdala and dorsal hippocampus of rats that were re-exposed to alcohol after a period of abstinence. Previous studies using similar animal models also demonstrated that changes in microglial morphology in brain (hippocampus, cortex, corpus callosum, cerebellum) associated with alcohol exposure consist of short, thick, few processes and large, irregular soma [51,52,55-58]. In the healthy brain, activated nature of resting microglia consist of multiple thin, branched processes with

dynamic movements towards synapses, checking the extracellular environment for possible threats [59]. However, a hyper-ramified state of microglia occurs in a context of pathological signals (cytokines and free radicals) induced by pathogens, neuronal damage or inflammation, and consist of secondary branching and rapid, stereotyped changes in process length and reorientation towards injury [60]. Fully activated state of microglia is characterized by a shortening and thickening in branched processes and an enlargement of the soma in an amoeboid appearance [61]. In the present study, we performed an in-depth quantitative analysis of morphometric parameters that discriminate successive changes in microglia morphology linked to different states of activation including spatial complexity (fractal dimension), heterogeneity (lacunarity), cell area, perimeter and circularity, and thickening/shortening (density and roughness) in the ramification patterns of the microglial processes. Particularly, fractal dimension seems a highly-sensitive index for detecting subtle, dynamic changes in response to a diffuse injury [62]. Our analysis of microglial morphology indicates that alcohol drinking reinstatement increases microglial process complexity and thickening, specifically present in the striatum and hippocampal CA1, and reduces microglial heterogeneity (smaller gaps in space between branches), specifically present in the prelimbic cortex and hippocampal CA1, suggesting a state of activated microglia.

Microglial cells are important in generating and maintaining neuroinflammatory responses [60]. Activated microglia are associated with the increased expression of innate immune toll-like receptors and the specific secretion of inflammatory factors [63], and these signals are capable of promoting proliferation and migration of neuroimmune cells in order to allow a brain region-specific immune response [64]. Pro-inflammatory cytokines including the interleukins IL1β and IL6, tumor necrosis factor alpha (TNFα), and transforming growth factors beta (TGFβ), as well as anti-inflammatory factors including the interleukins IL4, IL10 and the brain-derived neurotrophic factor (BDNF), ideally modulate the homeostatic inflammatory response to damage by removing pathogens or apoptotic cells [54]. However, long-term activation of microglia secreting inflammatory cytokines (or the imbalance between pro-inflammatory and anti-inflammatory cytokines) may contribute to the pathologic condition of AUD [31].

Among the neuropsychiatric disorders involving behavioral and cognitive dysfunction, depression is the most prevalent comorbidity in AUD patients. Similar to alcohol actions, over-activation of the neuroimmune system and microglial mechanisms that contribute to inflammation play a critical role in major depressive disorders [65]. Expression of the microglial marker IBA-1 and inflammatory cytokines (IL1β, TNFα, BDNF) are up-regulated in the brain of patients with major depression [65,66] and in animal models of depressive-like behavior [67,68]. Whether inflammation promotes susceptibility to depression, controlling inflammation by antidepressants may provide a comprehensive therapeutic benefit [69]. However, conventional SSRI antidepressants fail to respond to immunotherapies involving depressive disorder, demonstrating no, anti- or even pro-inflammatory effects [39-41,68,70]. Experimental studies reflecting the incongruence of clinical outcomes hypothesize that an interplay between SSRIs and the quality of the environmental conditions [35,71] may support the divergent effects of SSRI treatment on the inflammatory response [42,72-74]. Regarding our findings on microglial morphology, fluoxetine treatment cessation induced subtle changes in main morphometric parameters that indicate higher spatial complexity (fractal dimension) and lower heterogeneity (lacunarity), as well as increases in

process thickening and shortening (density and roughness), effects that are also more prominent in the striatum and hippocampal CA1. Together, these morphological changes suggest an increase in process branching and complexity that depicts a hyper-ramified, reactive state of microglia associated with fluoxetine treatment cessation, suggesting a microglial behavior that can be functionally over-reactive to that induced by alcohol.

Besides microglial morphology, our investigation also evidences that alcohol drinking reinstatement may contribute to support an imbalanced inflammatory response of SSRI antidepressants after the abrupt cessation of treatment during alcohol abstinence. Results indicate that fluoxetine treatment cessation in rats with alcohol drinking reinstatement is associated with changes in the expressions of both pro-inflammatory and anti-inflammatory cytokines (*TNFα*, *IL1β*, *IL*6, *IL4*, *IL10*, *TGFβ*, *BDNF*), most of the chemokines (*Cxcl12*, *Ccl2, Cx3cl1*) and *TLR4* in a brain region-specific manner, having the dorsal hippocampus a more significant neuroimmune response. It is of particular interest the lower mRNA expression of the pro-inflammatory chemokine *Cx3cl1* (*fractalkine*) in the PrL, BLA and dorsal hippocampus, as well as the higher mRNA expression of *TLR4* in the Str and dorsal hippocampus of those ethanol-exposed rats whose fluoxetine treatment was abruptly ceased. We next wonder whether fluoxetine-induced changes in inflammatory factors and *TLR4* are tightly related to microglial morphology. Overall, we found that an altered mRNA expression, induced by fluoxetine, in most of the inflammatory factors correlates with increases in fractal dimension (*D*), a morphological index of microglial spatial complexity (**Fig. 8**). Fractal dimension is a highly-sensitive parameter that mirrors secondary branching and process readjusting usually observed during the hyper-ramified state of the activated microglia [60]. Interestingly, we highlight that fluoxetine-induced decreases in *Cx3cl1* correlates with fractal dimension (spatial complexity) in the PrL and BLA, and microglial cell area (process branching) in the dorsal hippocampus of ethanol-exposed rats. The inverse association between *Cx3cl1* expression and spatial complexity and cell area of microglia agrees with the recently known role of CX3CL1 signaling on microglia-mediated synapse remodeling [75] and the subsequent declines in cognitive behavior in mice lacking *Cx3cl1* [76]. Moreover, microglial cell area correlates with fluoxetine-induced increases in the remaining chemokines (*Cxcl2*, *Ccl2*) and most of the inflammatory cytokines (*IL1β*, *IL6*, *IL10*) in the dorsal hippocampus. Moreover, in the dorsal hippocampus (**Fig. 8**), *TLR4* mRNA expression positively correlates with microglial cell area. It is of particular relevance that fluoxetine-induced increases in striatal *TLR4* specifically correlates with an increase in fractal dimension (D), a morphometric index that depicts complexity in process branching. The positive association between spatial complexity of microglia and *TLR4* expression support previous reports addressing a role of TLR4 receptors in microglial interactions with neurons including synaptic connections induced by ethanol [77]. Focusing on drinking behavior, these results also suggest that changes in microglial morphology and reactive phenotype, characterized by the expression of ethanol-specific TLR4 signaling of inflammatory and chemoattractant factors, may underlie fluoxetine-induced escalation of alcohol consumption as was previously described by our group [15,16]. Following this promising finding, further studies would be needed to determine whether the effect of SSRI antidepressants on microglial morphology linked to

TLR4/inflammatory signaling in the dorsal hippocampus may contribute to modulate cognitive impairment induced by long-term alcohol consumption.

There are some limitations on the present study that have to be highlighted. First, the data obtained using only male rats need to be extended towards females in order to confirm both fluoxetine cessation-induced escalation in alcohol consumption and the alterations in microglial reactivity described in the present study. The fact that fluoxetine activates anti-inflammatory mechanisms demands additional controls where the maintenance of fluoxetine treatment after resuming alcohol-self administration is present. Moreover, since fluoxetine induces escalation, a control pair-feeding with alcohol should be needed to identify dose effects. Finally, the apparent lack of direct effect of TLR4 signaling on ethanol excessive drinking [78] suggests the need of further studies to evaluate alternative mechanisms where the involvement of TLR4 in local neuroimmune/inflammatory responses may regulate ethanol-induced sedation via the histaminergic system [79].

In conclusion, our study provides evidence of brain region-specific effects of the SSRI fluoxetine treatment cessation on microglia morphology and neuroimmune/inflammatory response to alcohol drinking reinstatement. Data suggest that fluoxetine might modify neuroinflammation associated with alcohol consumption. They also remark the need to avoid abrupt cessation of fluoxetine that might produce relevant changes on neuroinflammatory mechanisms activated by alcohol intake, a fact that might be linked to the escalation of alcohol consumption and might also results in additional comorbidities. Results shed light on the complexity in understanding of the SSRI antidepressant actions on alcohol relapse, and may help to develop personalized strategies using SSRI antidepressants associated with anti-inflammatory medications as new therapeutic strategies for AUD and depression. Clinical studies using AUD patients with co-occurring depressive symptoms are needed to address the efficacy of these treatments.

Abbreviations

BCD, bounding circle diameter; BDNF, brain-derived neurotrophic factor; BLA, basolateral amygdala; CA, cell area; CA1/CA3, *cornu ammonis* subfields 1 and 3 of the hippocampus; CC, cell circularity; CCL2/MCP1, monocyte chemoattractant protein-1; CH, convex hull area (CHA), circularity (CHC), perimeter (CHP), and span ratio (CHSR); CP, cell perimeter; CX3CL1, fractalkine; CXCL12/SDF1, stromal cell derived factor 1; D, fractal dimension; DG, dentate gyrus of the hippocampus; Gapdh, glyceraldehyde-3-phosphate dehydrogenase; gcl, granular cell layer; IBA-1, allograph inflammaroty factor 1 or ionized calcium-binding adapter molecule 1; IL1β, interleukin 1 beta; IL4, interleukin 4; IL6, interleukin 6; IL10, interleukin 10; Lac, lacunarity (□); MR, the mean radius; MSACH, maximum span across the convex hull; pcl, polymorphic cell layer or hilus; PrL, prelimbic cortex (also known as medial prefrontal cortex); RCHR, the ratio maximum/minimum convex hull ratii; SR, stratum radiatum; Str, striatum; TGFB1, transforming growth factor beta 1; TLR4, toll-like receptor 4; TNFα, tumor necrosis factor.

Declarations

Funding

RETICS Red de Trastornos Adictivos, Instituto de Salud Carlos III (ISCIII), Ministerio de Ciencia e Innovación and European Regional Development Funds-European Union (ERDF-EU) (RD16/0017/0001); ISCIII, ERDF-EU (PI17/02026, PI19/01577); Ministerio de Sanidad, Delegación de Gobierno para el Plan Nacional sobre Drogas (PND 2020/048, PND 2019/040, PND 2018/044, PND 2018/033); and Consejería de Salud y Familia, Junta de Andalucía (*Neuro-RECA*, RIC-0111-2019). JS (CPII17/00024), FJP (CPII19/00022) and AS (CPII19/00031) hold “Miguel Servet II” research contracts from the National System of Health, ISCIII, ERDF-EU. FJP also holds a “Nicolas Monardes” contract from Servicio Andaluz de Salud, Consejería de Salud y Familia, Junta de Andalucía (C1-0049-2019). PR (CP19/00068) hold “Miguel Servet I” research contracts from the National System of Health, ISCIII, ERDF-EU. The funding sources had no further role in study design; in the collection, analysis and interpretation of data; in writing of the report; and in the decision to submit the paper for publication.

Conflict of Interest and Data Availability Statements

The authors declare that no competing interests exist. The data that support the findings of this study are available on reasonable request from the corresponding author.

Author Contributions

Conception and design: F.R.F., J.S. Data acquisition: J.A., M.M.F.-A., F.A., P.R. Data analysis and interpretation: J.A., F.J.P., A.S. Draft writing: J.A., F.R.F., J.S. Review and editing: L.R., I.S.-F., P.J.S.-C. Final approval: All authors.

References

1. Organization for Economic Co-operation and Development. OECD Health Statistics (2020) Non-Medical Determinants in Health: Alcohol consumption. http://www.oecd.org/els/health-systems/health-data.htm. Accessed to datasets in the 2020 online database at November, 4, 2020
2. Davidson KM (1995) Diagnosis of depression in alcohol dependence: changes in prevalence with drinking status. Br J Psychiatry 166:199–204. doi:10.1192/bjp.166.2.199
3. Fergusson DM, Boden JM, Horwood LJ (2009) Tests of causal links between alcohol abuse or dependence and major depression. Arch Gen Psychiatry 66:260–266. doi:10.1001/archgenpsychiatry.2008.543
4. Craske MG, Stein MB (2016) Anxiety Lancet 388:3048–3059. doi:10.1016/S0140-6736(16)30381-6
5. Ballesta A, Orio L, Arco R, Vargas A, Romero-Sanchiz P, Nogueira-Arjona R, de Heras RG, Antón M, Ramírez-López M, Serrano A, Pavón FJ, de Fonseca FR, Suárez J, Alen F (2019) Bupropion, a possible antidepressant without negative effects on alcohol relapse. Eur Neuropsychopharmacol 29:756–765. doi:10.1016/j.euroneuro.2019.03.012

6. Ballesta A, Alen F, Orio L, Arco R, Vadas E, Decara J, Vargas A, Gómez de Heras R, Ramírez-López M, Serrano A, Pavón FJ, Suárez J, Rodríguez de Fonseca F (2020) Abrupt cessation of reboxetine along alcohol deprivation results in alcohol intake escalation after reinstatement of drinking. Addict Biol 20:e12957. doi:10.1111/adb.12957
7. Torrens M, Fonseca F, Mateu G, Farré M (2005) Efficacy of antidepressants in substance use disorders with and without comorbid depression. A systematic review and meta-analysis. Drug Alcohol Depend 78:1–22. doi:10.1016/j.drugalcdep.2004.09.004
8. Uzbay IT (2008) Serotonergic anti-depressants and ethanol withdrawal syndrome: a review. Alcohol Alcohol 43:15–24. doi:10.1093/alcalc/agm145
9. Simon O'Brien, Legastelois E, Houchi R, Vilpoux H, Alaux-Cantin C, Pierrefiche S, André O, Naassila E M (2011) Fluoxetine, desipramine, and the dual antidepressant milnacipran reduce alcohol self-administration and/or relapse in dependent rats. Neuropsychopharmacology 36:1518–1530. doi:10.1038/npp.2011.37
10. Bell RL, Hauser SR, Liang T, Sari Y, Maldonado-Devincci A, Rodd ZA (2017) Rat animal models for screening medications to treat alcohol use disorders. Neuropharmacology 122:201–243. doi:10.1016/j.neuropharm.2017.02.004
11. Agabio R, Trogu E, Pani PP (2018) Antidepressants for the treatment of people with co-occurring depression and alcohol dependence. Cochrane Database Syst Rev 4:CD008581. doi:10.1002/14651858.CD008581.pub2
12. Ch'Ng SS, Lawrence AJ (2018) Investigational drugs for alcohol use disorders: a review of preclinical data. Expert Opin Investig Drugs 27:459–474. doi:10.1080/13543784.2018.1472763
13. Ray LA, Bujarski S, Roche DJO, Magill M (2018) Overcoming the "Valley of Death" in Medications Development for Alcohol Use Disorder. Alcohol Clin Exp Res 42:1612–1622. doi:10.1111/acer.13829
14. Kranzler HR, Burleson JA, Brown J, Babor TF (1996) Fluoxetine treatment seems to reduce the beneficial effects of cognitive-behavioral therapy in type B alcoholics. Alcohol Clin Exp Res 20:1534–1541. doi:10.1111/j.1530-0277.1996.tb01696.x
15. Alén F, Orio L, Gorriti M, de Heras RG, Ramírez-López MT, Pozo M, de Fonseca FR (2013) Increased alcohol consumption in rats after subchronic antidepressant treatment. Int J Neuropsychopharmacol 16:1809–1818. doi:10.1017/S1461145713000217
16. Suárez J, Khom S, Alén F, Natividad LA, Varodayan FP, Patel RR, Kirson D, Arco R, Ballesta A, Bajo M, Rubio L, Martin-Fardon R, Rodríguez de Fonseca F, Roberto M (2020) Cessation of fluoxetine treatment increases alcohol seeking during relapse and dysregulates endocannabinoid and glutamatergic signaling in the central amygdala. Addict Biol 25:e12813. doi:10.1111/adb.12813
17. Crews FT, Sarkar DK, Qin L, Zou J, Boyadjieva N, Vetreno RP (2015) Neuroimmune Function and the Consequences of Alcohol Exposure. Alcohol Res 37:331–341, 344 – 51
18. Montesinos J, Alfonso-Loeches S, Guerri C (2016) Impact of the Innate Immune Response in the Actions of Ethanol on the Central Nervous System. Alcohol Clin Exp Res 40:2260–2270. doi:10.1111/acer.13208

19. Pascual M, Montesinos J, Guerri C (2018) Role of the innate immune system in the neuropathological consequences induced by adolescent binge drinking. J Neurosci Res 96:765–780. doi:10.1002/jnr.24203
20. Chastain LG, Sarkar DK (2014) Role of microglia in regulation of ethanol neurotoxic action. Int Rev Neurobiol 118:81–103. doi:10.1016/B978-0-12-801284-0.00004-X
21. Rivera P, Fernández-Arjona MDM, Silva-Peña D, Blanco E, Vargas A, López-Ávalos MD, Grondona JM, Serrano A, Pavón FJ, Rodríguez de Fonseca F, Suárez J (2018) Pharmacological blockade of fatty acid amide hydrolase (FAAH) by URB597 improves memory and changes the phenotype of hippocampal microglia despite ethanol exposure. Biochem Pharmacol 157:244–257. doi:10.1016/j.bcp.2018.08.005
22. Montesinos J, Pascual M, Pla A, Maldonado C, Rodríguez-Arias M, Miñarro J, Guerri C (2015) TLR4 elimination prevents synaptic and myelin alterations and long- term cognitive dysfunctions in adolescent mice with intermittent ethanol treatment. Brain Behav Immun 45:233–244. doi:10.1016/j.bbi.2014.11.015
23. Antón M, Alén F, Gómez de Heras R, Serrano A, Pavón FJ, Leza JC, García-Bueno B, Rodríguez de Fonseca F, Orio L (2017) Oleoylethanolamide prevents neuroimmune HMGB1/TLR4/NF-kB danger signaling in rat frontal cortex and depressive-like behavior induced by ethanol binge administration. Addict Biol 22:724–741. doi:10.1111/adb.12365
24. Boyadjieva NI, Sarkar DK (2010) Role of microglia in ethanol's apoptotic action on hypothalamic neuronal cells in primary cultures. Alcohol Clin Exp Res 34:1835–1842. doi:10.1111/j.1530-0277.2010.01271.x
25. Alfonso-Loeches S, Guerri C (2011) Molecular and behavioral aspects of the actions of alcohol on the adult and developing brain. Crit Rev Clin Lab Sci 48:19–47. doi:10.3109/10408363.2011.580567
26. Guadagno J, Xu X, Karajgikar M, Brown A, Cregan SP (2013) Microglia-derived TNFα induces apoptosis in neural precursor cells via transcriptional activation of the Bcl-2 family member Puma. Cell Death Dis 4:e538. doi:10.1038/cddis.2013.59
27. Morris SA, Eaves DW, Smith AR, Nixon K (2010) Alcohol inhibition of neurogenesis: a mechanism of hippocampal neurodegeneration in an adolescent alcohol abuse model. Hippocampus 20:596–607. doi:10.1002/hipo.20665
28. García Bueno B, Caso JR, Madrigal JL, Leza JC (2016) Innate immune receptor Toll-like receptor 4 signalling in neuropsychiatric diseases. Neurosci Biobehav Rev 64:134–147. doi:10.1016/j.neubiorev.2016.02.013
29. Medina-Rodríguez EM, Rice KC, Beurel E, Jope RS (2020) (+)-Naloxone blocks Toll-like receptor 4 to ameliorate deleterious effects of stress on male mouse behaviors. Brain Behav Immun 26:S0889-1591(20)31219-8. doi: 10.1016/j.bbi.2020.08.022
30. Zhang K, Lin W, Zhang J, Zhao Y, Wang X, Zhao M (2020) Effect of Toll-like receptor 4 on depressive-like behaviors induced by chronic social defeat stress. Brain Behav 10:e01525. doi:10.1002/brb3.1525

31. Crews FT, Zou J, Qin L (2011) Induction of innate immune genes in brain create the neurobiology of addiction. Brain Behav Immun 25(Suppl 1):S4–S12. doi:10.1016/j.bbi.2011.03.003
32. Ehrlich D, Pirchl M, Humpel C (2012) Effects of long-term moderate ethanol and cholesterol on cognition, cholinergic neurons, inflammation, and vascular impairment in rats. Neuroscience 205:154–166. doi:10.1016/j.neuroscience.2011.12.054
33. Lee JY, Kang SR, Yune TY (2015) Fluoxetine prevents oligodendrocyte cell death by inhibiting microglia activation after spinal cord injury. J Neurotrauma 32:633–644. doi:10.1089/neu.2014.3527
34. Liechti FD, Grandgirard D, Leib SL (2015) The antidepressant fluoxetine protects the hippocampus from brain damage in experimental pneumococcal meningitis. Neuroscience 297:89–94. doi:10.1016/j.neuroscience.2015.03.056
35. Alboni S, Poggini S, Garofalo S, Milior G, El Hajj H, Lecours C, Girard I, Gagnon S, Boisjoly-Villeneuve S, Brunello N, Wolfer DP, Limatola C, Tremblay M, Maggi L, Branchi I (2016) Fluoxetine treatment affects the inflammatory response and microglial function according to the quality of the living environment. Brain Behav Immun 58:261–271. doi:10.1016/j.bbi.2016.07.155
36. Khodanovich M, Kisel A, Kudabaeva M, Chernysheva G, Smolyakova V, Krutenkova E, Wasserlauf I, Plotnikov M, Yarnykh V (2018) Effects of Fluoxetine on Hippocampal Neurogenesis and Neuroprotection in the Model of Global Cerebral Ischemia in Rats. Int J Mol Sci 19:162. doi:10.3390/ijms19010162
37. Liu FY, Cai J, Wang C, Ruan W, Guan GP, Pan HZ, Li JR, Qian C, Chen JS, Wang L, Chen G (2018) Fluoxetine attenuates neuroinflammation in early brain injury after subarachnoid hemorrhage: a possible role for the regulation of TLR4/MyD88/NF-κB signaling pathway. J Neuroinflammation 15:347. doi:10.1186/s12974-018-1388-x
38. Yoshimura R, Hori H, Ikenouchi-Sugita A, Umene-Nakano W, Ueda N, Nakamura J (2009) Higher plasma interleukin-6 (IL-6) level is associated with SSRI- or SNRI-refractory depression. Prog Neuropsychopharmacol Biol Psychiatry 33:722–726. doi:10.1016/j.pnpbp.2009.03.020
39. Hannestad J, DellaGioia N, Bloch M (2011) The effect of antidepressant medication treatment on serum levels of inflammatory cytokines: a meta-analysis. Neuropsychopharmacology 36:2452–2459. doi:10.1038/npp.2011.132
40. Kim JW, Kim YK, Hwang JA, Yoon HK, Ko YH, Han C, Lee HJ, Ham BJ, Lee HS (2013) Plasma Levels of IL-23 and IL-17 before and after Antidepressant Treatment in Patients with Major Depressive Disorder. Psychiatry Investig 10:294–299. doi:10.4306/pi.2013.10.3.294
41. Chen CY, Yeh YW, Kuo SC, Liang CS, Ho PS, Huang CC, Yen CH, Shyu JF, Lu RB, Huang SY (2018) Differences in immunomodulatory properties between venlafaxine and paroxetine in patients with major depressive disorder. Psychoneuroendocrinology 87:108–118. doi:10.1016/j.psyneuen.2017.10.009
42. Tynan RJ, Weidenhofer J, Hinwood M, Cairns MJ, Day TA, Walker FR (2012) A comparative examination of the anti-inflammatory effects of SSRI and SNRI antidepressants on LPS stimulated

microglia. Brain Behav Immun 26:469–479. doi:10.1016/j.bbi.2011.12.011

43. Vengeliene V, Bilbao A, Spanagel R (2014) The alcohol deprivation effect model for studying relapse behavior: a comparison between rats and mice. Alcohol 48:313–320. doi:10.1016/j.alcohol.2014.03.002
44. Paxinos G, Watson C (2007) The Rat Brain in Stereotaxic Coordinates, 6th edn. Academic Press; Elsevier, New York
45. Fernández-Arjona MDM, Grondona JM, Granados-Durán P, Fernández-Llebrez P, López-Ávalos MD (2017) Microglia Morphological Categorization in a Rat Model of Neuroinflammation by Hierarchical Cluster and Principal Components Analysis. Front Cell Neurosci 11:235. doi:10.3389/fncel.2017.00235
46. Karperien A, Ahammer H, Jelinek HF (2013) Quantitating the subtleties of microglial morphology with fractal analysis. Front Cell Neurosci 7:3. doi:10.3389/fncel.2013.00003
47. Neupane SP (2016) Neuroimmune Interface in the Comorbidity between Alcohol Use Disorder and Major Depression. Front Immunol 7:655. doi:10.3389/fimmu.2016.00655
48. Erickson EK, Grantham EK, Warden AS, Harris RA (2019) Neuroimmune signaling in alcohol use disorder. Pharmacol Biochem Behav 177:34–60. doi:10.1016/j.pbb.2018.12.007
49. Alfonso-Loeches S, Pascual-Lucas M, Blanco AM, Sanchez-Vera I, Guerri C (2010) Pivotal role of TLR4 receptors in alcohol-induced neuroinflammation and brain damage. J Neurosci 30:8285–8295. doi:10.1523/JNEUROSCI.0976-10.2010
50. Ohsawa K, Imai Y, Sasaki Y, Kohsaka S (2004) Microglia/macrophage-specific protein Iba1 binds to fimbrin and enhances its actin-bundling activity. J Neurochem 88:844–856. doi:10.1046/j.1471-4159.2003.02213.x
51. Saito M, Chakraborty G, Mao RF, Paik SM, Vadasz C, Saito M (2010) Tau phosphorylation and cleavage in ethanol-induced neurodegeneration in the developing mouse brain. Neurochem Res 35:651–659. doi:10.1007/s11064-009-0116-4
52. Qin L, Crews FT (2012) Chronic ethanol increases systemic TLR3 agonist-induced neuroinflammation and neurodegeneration. J Neuroinflammation 9:130. doi:10.1186/1742-2094-9-130
53. Qin L, Crews FT (2012) NADPH oxidase and reactive oxygen species contribute to alcohol-induced microglial activation and neurodegeneration. J Neuroinflammation 9:5. doi:10.1186/1742-2094-9-5
54. Marshall SA, McClain JA, Kelso ML, Hopkins DM, Pauly JR, Nixon K (2013) Microglial activation is not equivalent to neuroinflammation in alcohol-induced neurodegeneration: The importance of microglia phenotype. Neurobiol Dis 54:239–251. doi:10.1016/j.nbd.2012.12.016
55. Ward RJ, Colivicchi MA, Allen R, Schol F, Lallemand F, de Witte P, Ballini C, Corte LD, Dexter D (2009) Neuro-inflammation induced in the hippocampus of 'binge drinking' rats may be mediated by elevated extracellular glutamate content. J Neurochem 111:1119–1128. doi:10.1111/j.1471-4159.2009.06389.x

56. Kane CJ, Phelan KD, Han L, Smith RR, Xie J, Douglas JC, Drew PD (2011) Protection of neurons and microglia against ethanol in a mouse model of fetal alcohol spectrum disorders by peroxisome proliferator-activated receptor-γ agonists. Brain Behav Immun 25(Suppl 1):S137–S145. doi:10.1016/j.bbi.2011.02.016
57. McClain JA, Morris SA, Deeny MA, Marshall SA, Hayes DM, Kiser ZM, Nixon K (2011) Adolescent binge alcohol exposure induces long-lasting partial activation of microglia. Brain Behav Immun 25(Suppl 1):S120–S128. doi:10.1016/j.bbi.2011.01.006
58. Zhao YN, Wang F, Fan YX, Ping GF, Yang JY, Wu CF (2013) Activated microglia are implicated in cognitive deficits, neuronal death, and successful recovery following intermittent ethanol exposure. Behav Brain Res 236:270–282. doi:10.1016/j.bbr.2012.08.052
59. Tremblay M, Stevens B, Sierra A, Wake H, Bessis A, Nimmerjahn A (2011) The role of microglia in the healthy brain. J Neurosci 31:16064–16069. doi:10.1523/JNEUROSCI.4158-11.2011
60. Beynon SB, Walker FR (2012) Microglial activation in the injured and healthy brain: what are we really talking about? Practical and theoretical issues associated with the measurement of changes in microglial morphology. Neuroscience 225:162–171. doi:10.1016/j.neuroscience.2012.07.029
61. Kreutzberg GW (1996) Microglia: a sensor for pathological events in the CNS. Trends Neurosci 19:312–318. doi:10.1016/0166-2236(96)10049-7
62. Soltys Z, Ziaja M, Pawlínski R, Setkowicz Z, Janeczko K (2001) Morphology of reactive microglia in the injured cerebral cortex. Fractal analysis and complementary quantitative methods. J Neurosci Res 63:90 – 7. doi: 10.1002/1097-4547(20010101)63:1<90::AID-JNR11>3.0.CO;2-9.
63. Suzumura A (2009) [Neurotoxicity by microglia: the mechanisms and potential therapeutic strategy]. Fukuoka Igaku Zasshi 100:243–247
64. Badoer E. Microglia: activation in acute and chronic inflammatory states and in response to cardiovascular dysfunction (2010) Int J Biochem Cell Biol 42:1580–5. doi: 10.1016/j.biocel.2010.07.005
65. Rahman S, Alzarea S (2019) Glial mechanisms underlying major depressive disorder: Potential therapeutic opportunities. Prog Mol Biol Transl Sci 167:159–178. doi:10.1016/bs.pmbts.2019.06.010
66. Torres-Platas SG, Cruceanu C, Chen GG, Turecki G, Mechawar N (2014) Evidence for increased microglial priming and macrophage recruitment in the dorsal anterior cingulate white matter of depressed suicides. Brain Behav Immun 42:50–59. doi:10.1016/j.bbi.2014.05.007
67. Kreisel T, Frank MG, Licht T, Reshef R, Ben-Menachem-Zidon O, Baratta MV, Maier SF, Yirmiya R (2014) Dynamic microglial alterations underlie stress-induced depressive-like behavior and suppressed neurogenesis. Mol Psychiatry 19:699–709. doi:10.1038/mp.2013.155
68. Tomaz VS, Chaves Filho AJM, Cordeiro RC, Jucá PM, Soares MVR, Barroso PN, Cristino LMF, Jiang W, Teixeira AL, de Lucena DF, Macedo DS (2020) Antidepressants of different classes cause distinct behavioral and brain pro- and anti-inflammatory changes in mice submitted to an inflammatory model of depression. J Affect Disord 268:188–200. doi:10.1016/j.jad.2020.03.022

69. Beurel E, Toups M, Nemeroff CB (2020) The Bidirectional Relationship of Depression and Inflammation: Double Trouble. Neuron 107:234–256. doi:10.1016/j.neuron.2020.06.002
70. Yoshimura R, Hori H, Ikenouchi-Sugita A, Umene-Nakano W, Katsuki A, Atake K, Nakamura J (2013) Plasma levels of interleukin-6 and selective serotonin reuptake inhibitor response in patients with major depressive disorder. Hum Psychopharmacol 28:466–470. doi:10.1002/hup.2333
71. Alboni S, van Dijk RM, Poggini S, Milior G, Perrotta M, Drenth T, Brunello N, Wolfer DP, Limatola C, Amrein I, Cirulli F, Maggi L, Branchi I (2017) Fluoxetine effects on molecular, cellular and behavioral endophenotypes of depression are driven by the living environment. Mol Psychiatry 22:552–561. doi:10.1038/mp.2015.142
72. Horowitz MA, Wertz J, Zhu D, Cattaneo A, Musaelyan K, Nikkheslat N, Thuret S, Pariante CM, Zunszain PA (2014) Antidepressant compounds can be both pro- and anti-inflammatory in human hippocampal cells. Int J Neuropsychopharmacol 18:pyu076. doi:10.1093/ijnp/pyu076
73. Lu Y, Ho CS, Liu X, Chua AN, Wang W, McIntyre RS, Ho RC (2017) Chronic administration of fluoxetine and pro-inflammatory cytokine change in a rat model of depression. PLoS One 12:e0186700. doi:10.1371/journal.pone.0186700
74. Zhang X, Yin Y, Yue L, Gong L (2019) Selective Serotonin Reuptake Inhibitors Aggravate Depression-Associated Dry Eye Via Activating the NF-κB Pathway. Invest Ophthalmol Vis Sci 60:407–419. doi:10.1167/iovs.18-25572
75. Gunner G, Cheadle L, Johnson KM, Ayata P, Badimon A, Mondo E, Nagy MA, Liu L, Bemiller SM, Kim KW, Lira SA, Lamb BT, Tapper AR, Ransohoff RM, Greenberg ME, Schaefer A, Schafer DP (2019) Sensory lesioning induces microglial synapse elimination via ADAM10 and fractalkine signaling. Nat Neurosci 22:1075–1088. doi:10.1038/s41593-019-0419-y
76. Winter AN, Subbarayan MS, Grimmig B, Weesner JA, Moss L, Peters M, Weeber E, Nash K, Bickford PC (2020) Two forms of CX3CL1 display differential activity and rescue cognitive deficits in CX3CL1 knockout mice. J Neuroinflammation 17:157. doi:10.1186/s12974-020-01828-y
77. Montesinos J, Pascual M, Millán-Esteban D, Guerri C (2018) Binge-like ethanol treatment in adolescence impairs autophagy and hinders synaptic maturation: Role of TLR4. Neurosci Lett 682:85–91. doi:10.1016/j.neulet.2018.05.049
78. Harris RA, Bajo M, Bell RL, Blednov YA, Varodayan FP, Truitt JM, de Guglielmo G, Lasek AW, Logrip ML, Vendruscolo LF, Roberts AJ, Roberts E, George O, Mayfield J, Billiar TR, Hackam DJ, Mayfield RD, Koob GF, Roberto M, Homanics GE (2017) Genetic and Pharmacologic Manipulation of TLR4 Has Minimal Impact on Ethanol Consumption in Rodents. J Neurosci 37:1139–1155. doi:10.1523/JNEUROSCI.2002-16.2016
79. Ma Z, Wang W, Wang T, Xu W, Qu W, Huang Z, Hong Z (2019) Ethanol Induces Sedation and Hypnosis via Inhibiting Histamine Release in Mice. Neurochem Res 44:1764–1772. doi:10.1007/s11064-019-02813-5

Tables

Table 1. Primer references for TaqMan® Gene Expression Assays (ThermoFisher)

Gene ID	GenBank accession numbers	Assay ID	Amplicon length
CX3CL1 (Fractalkine)	NM_134455.1	Rn00593186_m1	74
CXCL12 (SDF1)	NM_001033882.1	Rn00573260_m1	60
CCL2 (MCP-1)	NM_031530.1	Rn00580555_m1	95
TNFα	NM_012675.3	Rn01525859_g1	92
IL1β	NM_031512.2	Rn00580432_m1	74
IL-6	NM_012589.2	Rn01410330_m1	121
IL-4	NM_201270.1	Rn01456866_m1	128
IL-10	NM_012854.2	Rn01483988_g1	105
TGFB1	NM_021578.2	Rn00572010_m1	65
BDNF	NM_001270630.1	Rn02531967_s1	142
TLR4	NM_019178.1	Rn00569848_m1	127
Gadph	NM_017008.4	Rn01775763_g1	174

Abbreviations: BDNF, Brain-Derived Neurotrophic factor; CCL2/MCP1, Monocyte Chemoattractant Protein-1; CX3CL1, Fractalkine; CXCL12/SDF1, Stromal Cell Derived Factor 1; Gapdh, Glyceraldehyde-3-Phosphate Dehydrogenase; IL1β, Interleukin 1 beta; IL-4, Interleukin 4; IL-6, Interleukin 6; IL-10, Interleukin 10; TGFB1, Transforming Growth Factor Beta 1; TLR4, Toll-like Receptor 4; TNFα, Tumor Necrosis Factor.

Table 2. Interaction and effects of drinking (saccharine *vs*. ethanol) and treatment (vehicle *vs*. fluoxetine) on morphometric parameters of microglial cells expressing IBA-1.

Morphometric parameters	Two-way ANOVA	Prelimbic cortex (PrL)	Striatum (Str)	Basolateral amygdala (BLA)	Hippocampal CA1 region
Fractal dimension (D)	Interaction	*ns*[a]	*ns*	*ns*	$F_{1,196}$=5.93, *P*<.02
	Drinking	$F_{1,196}$=4.88, *P*<.03	$F_{1,196}$=11.2, *P*<.001	*ns*	$F_{1,196}$=6.10, *P*<.02
	Treatment	*ns*	$F_{1,196}$=6.34, *P*<.02	*ns*	$F_{1,196}$=4.65, *P*<.03
Lacunarity (□)	Interaction	*ns*	*ns*	*ns*	$F_{1,196}$=13.9, *P*<.001
	Drinking	$F_{1,196}$=12.1, *P*<.001	*ns*	$F_{1,196}$=3.75, *P*=.05	*ns*
	Treatment	*ns*	*ns*	*ns*	*ns*
Cell area (CA)	Interaction	*ns*	*ns*	*ns*	*ns*
	Drinking	$F_{1,196}$=7.27, *P*<.01	$F_{1,196}$=18.4, *P*<.000	*ns*	$F_{1,196}$=25.4, *P*<.000
	Treatment	*ns*	*ns*	*ns*	*ns*
Cell perimeter (CP)	Interaction	*ns*	*ns*	$F_{1,196}$=3.13, *P*=.07	*ns*
	Drinking	$F_{1,196}$=7.67, *P*<.01	$F_{1,196}$=10.8, *P*<.001	*ns*	$F_{1,196}$=21.2, *P*<.000
	Treatment	*ns*	$F_{1,196}$=4.19, *P*<.04	*ns*	*ns*
Cell circularity (CC)	Interaction	*ns*	$F_{1,196}$=4.25, *P*<.04	$F_{1,196}$=4.49, *P*<.03	*ns*
	Drinking	$F_{1,196}$=9.42, *P*<.01	$F_{1,196}$=11.1, *P*<.001	*ns*	*ns*
	Treatment	*ns*	$F_{1,196}$=4.69, *P*<.03	*ns*	$F_{1,196}$=11.2, *P*<.001
Convex hull area (CHA)	Interaction	*ns*	*ns*	$F_{1,196}$=3.69, *P*=.05	*ns*
	Drinking	*ns*	$F_{1,196}$=5.00, *P*<.03	*ns*	$F_{1,196}$=11.6, *P*<.001
	Treatment	*ns*	$F_{1,196}$=5.03, *P*<.03	*ns*	$F_{1,196}$=6.54, *P*<.02
Density (ρ)	Interaction	*ns*	*ns*	*ns*	$F_{1,196}$=11.4, *P*<.01
	Drinking	*ns*			

	Treatment	*ns*	$F_{1,196}$=8.77, *P*<.003	$F_{1,196}$=8.52, *P*<.004	*ns*
			ns	*ns*	$F_{1,196}$=5.38, *P*<.03
Convex hull perimeter (CHP)	Interaction	*ns*	*ns*	$F_{1,196}$=3.52, *P*=.06	*ns*
	Drinking	*ns*	$F_{1,196}$=5.84, *P*<.02	*ns*	$F_{1,196}$=6.96, *P*<.01
	Treatment	*ns*	$F_{1,196}$=4.20, *P*<.04	*ns*	$F_{1,196}$=6.76, *P*<.02
Roughness (R)	Interaction	$F_{1,196}$=4.10, *P*<.05	*ns*	*ns*	*ns*
	Drinking	$F_{1,196}$=8.15, *P*<.01	$F_{1,196}$=10.6, *P*<.002	*ns*	$F_{1,196}$=9.41, *P*<.003
	Treatment	*ns*	$F_{1,196}$=4.22, *P*<.04	*ns*	*ns*
Convex hull circularity (CHC)	Interaction	*ns*	*ns*	*ns*	*ns*
	Drinking	*ns*	$F_{1,196}$=4.05, *P*<.05	*ns*	*ns*
	Treatment	*ns*	*ns*	*ns*	$F_{1,196}$=34.4, *P*<.000
Convex hull span ratio (CHSR)	Interaction	*ns*	*ns*	*ns*	*ns*
	Drinking	*ns*	*ns*	*ns*	$F_{1,196}$=32.4, *P*<.000
	Treatment	*ns*	*ns*	*ns*	*ns*
Bounding circle diameter (BCD)	Interaction	*ns*	*ns*	*ns*	*ns*
	Drinking	*ns*	$F_{1,196}$=5.10, *P*<.03	*ns*	*ns*
	Treatment	$F_{1,196}$=6.10, *P*<.05	*ns*	*ns*	$F_{1,196}$=6.96, *P*<.01
Maximum span across the convex hull (MSACH)	Interaction	*ns*	*ns*	*ns*	*ns*
	Drinking	*ns*	$F_{1,196}$=4.98, *P*<.03	*ns*	*ns*
	Treatment	$F_{1,196}$=6.16, *P*<.05	*ns*	*ns*	$F_{1,196}$=6.74, *P*<.02
The ratio maximum/ minimum convex hull radii (RCHR)	Interaction	*ns*	*ns*	*ns*	*ns*
	Drinking	*ns*	*ns*	*ns*	$F_{1,196}$=26.3, *P*<.000
	Treatment	*ns*	*ns*	*ns*	*ns*

The mean radius (MR)	Interaction	*ns*	*ns*	*ns*	*ns*
	Drinking	*ns*	$F_{1,196}$=5.63, *P*<.02	*ns*	$F_{1,196}$=5.32, *P*<.03
	Treatment	$F_{1,196}$=4.36, *P*=.05	*ns*	*ns*	$F_{1,196}$=7.59, *P*<.007

[a]*ns, not significant.*

Figures

Figure 1

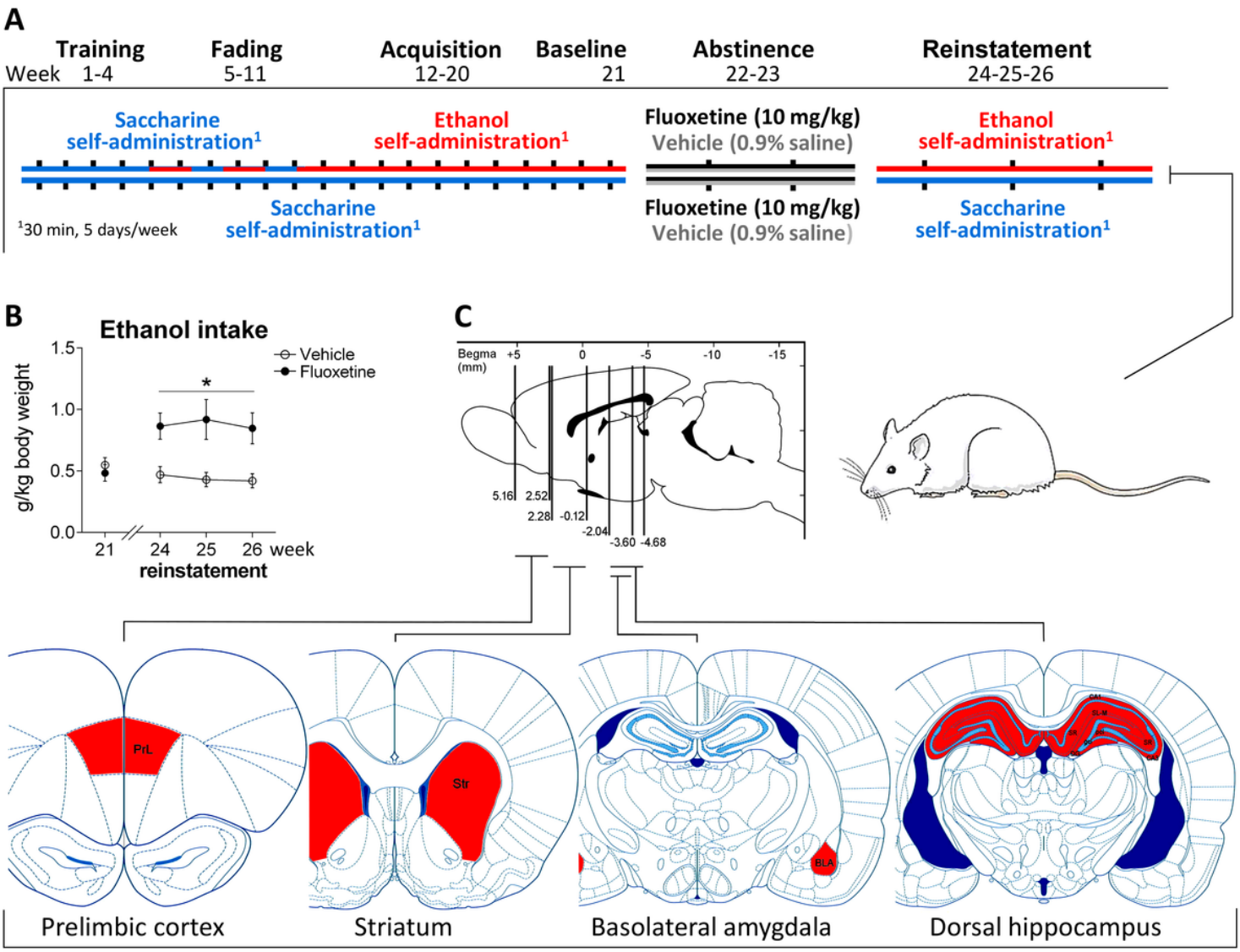

Figure 1

Schematic representation of the experiment. (A) Timeline of a paradigm of a rat model of ethanol self-administration showing stable ethanol drinking after 21 weeks of acquisition following abstinence and

fluoxetine treatment (10 mg/kg/day) for 14 days, and ethanol drinking reinstatement for 3 weeks. (B) Weekly average of ethanol intake (g/kg) were represented during ethanol self-administration baseline (week 21) and reinstatement (weeks 24-26). Tukey's test: *p < 0.05 vs. vehicle. (C) Schematic representation of the brain regions analyzed.

Figure 2

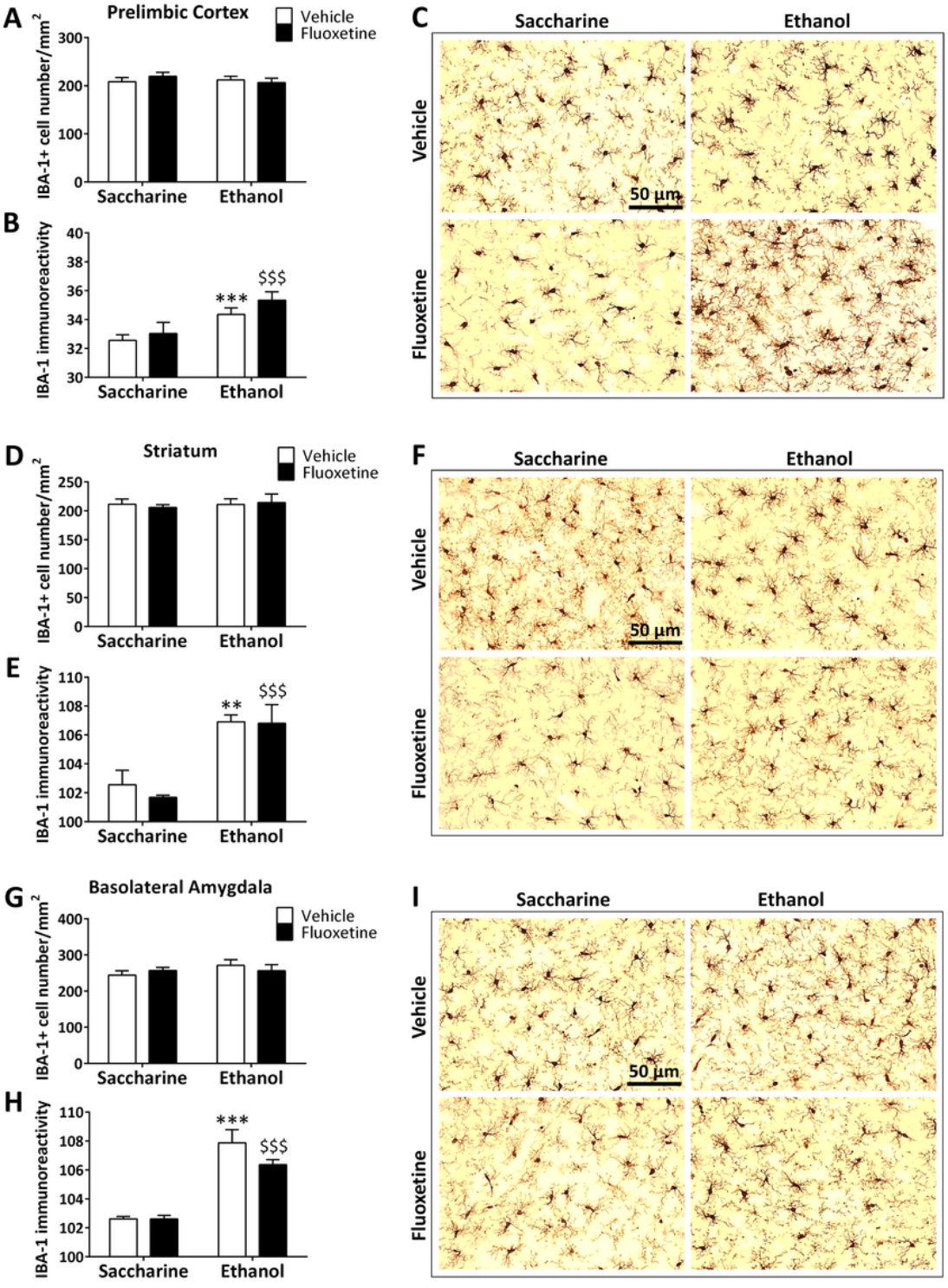

Figure 2

Effects of fluoxetine treatment cessation and ethanol drinking reinstatement on the number of IBA-1+ microglial cells and IBA-1 immunoreactivity in the prelimbic cortex (A, B), striatum (D, E) and basolateral amygdala (G, H). The histograms represent the mean + SEM of cells per area (mm2) and arbitrary units of immunoreactivity (n = 6 rats per experimental group). Tukey's test: **/***p < 0.01/0.001 vs. saccharine-vehicle group; $$$p < 0.001 vs. saccharine-fluoxetine group. Representative microphotographs showing magnification views of the immunostaining in the prelimbic cortex (C), striatum (F) and basolateral amygdala (I). Scale bars are included in representative images.

Figure 3

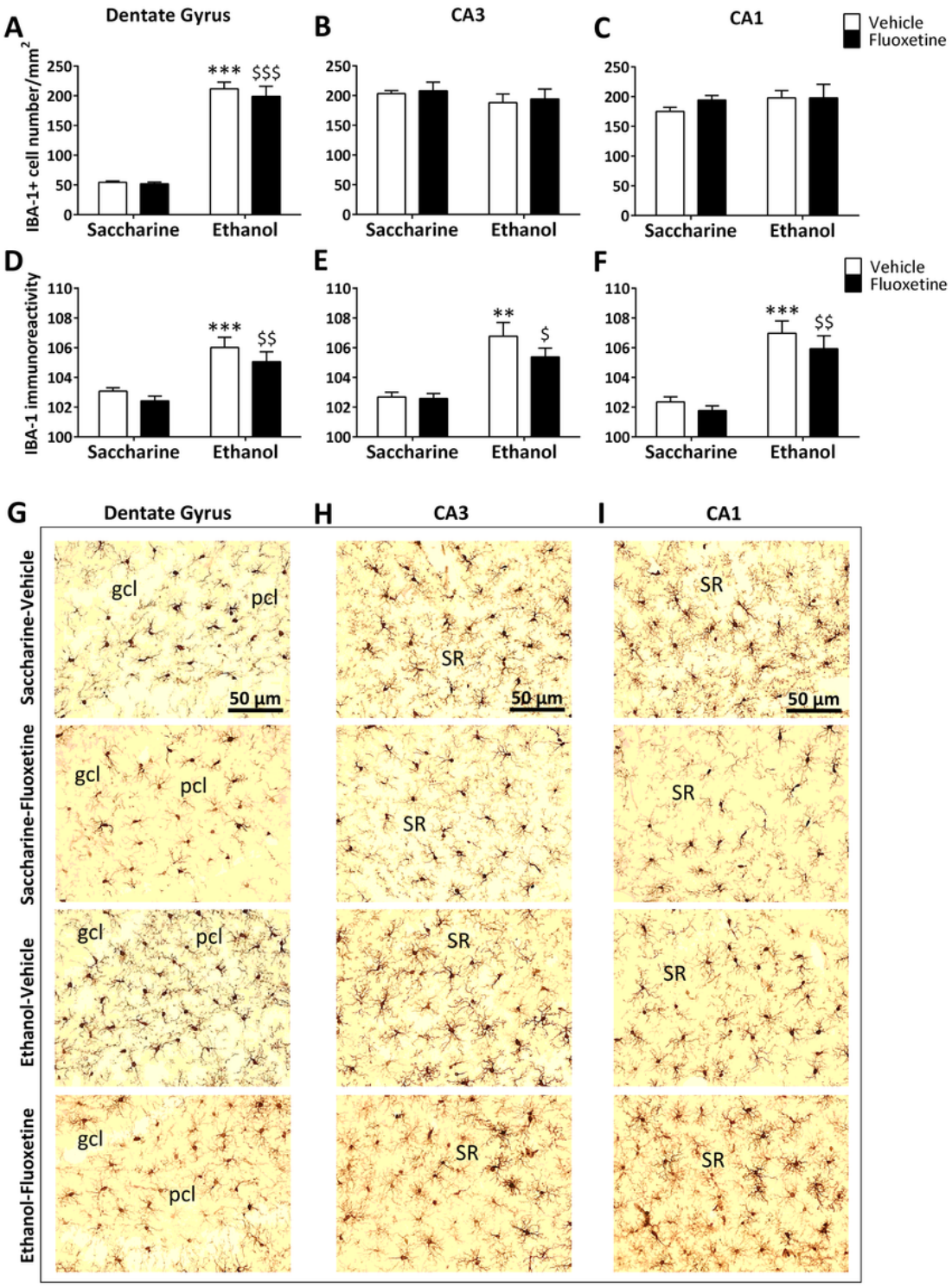

Figure 3

Effects of fluoxetine treatment cessation and ethanol drinking reinstatement on the number of IBA-1+ microglial cells and IBA-1 immunoreactivity in the dentate gyrus (A, D), and the hippocampal CA3 (B, E) and CA1 (C, F). The histograms represent the mean + SEM of cells per area (mm2) and arbitrary units of immunoreactivity (n = 6 rats per experimental group). Tukey's test: **/***p < 0.01/0.001 vs. saccharine-vehicle group; $/

/

$p < 0.05/0.01/0.001 vs. saccharine-fluoxetine group. Representative microphotographs showing magnification views of the immunostaining in the dentate gyrus (G), and the hippocampal CA3 (H) and CA1 (I). Scale bars are included in representative images.

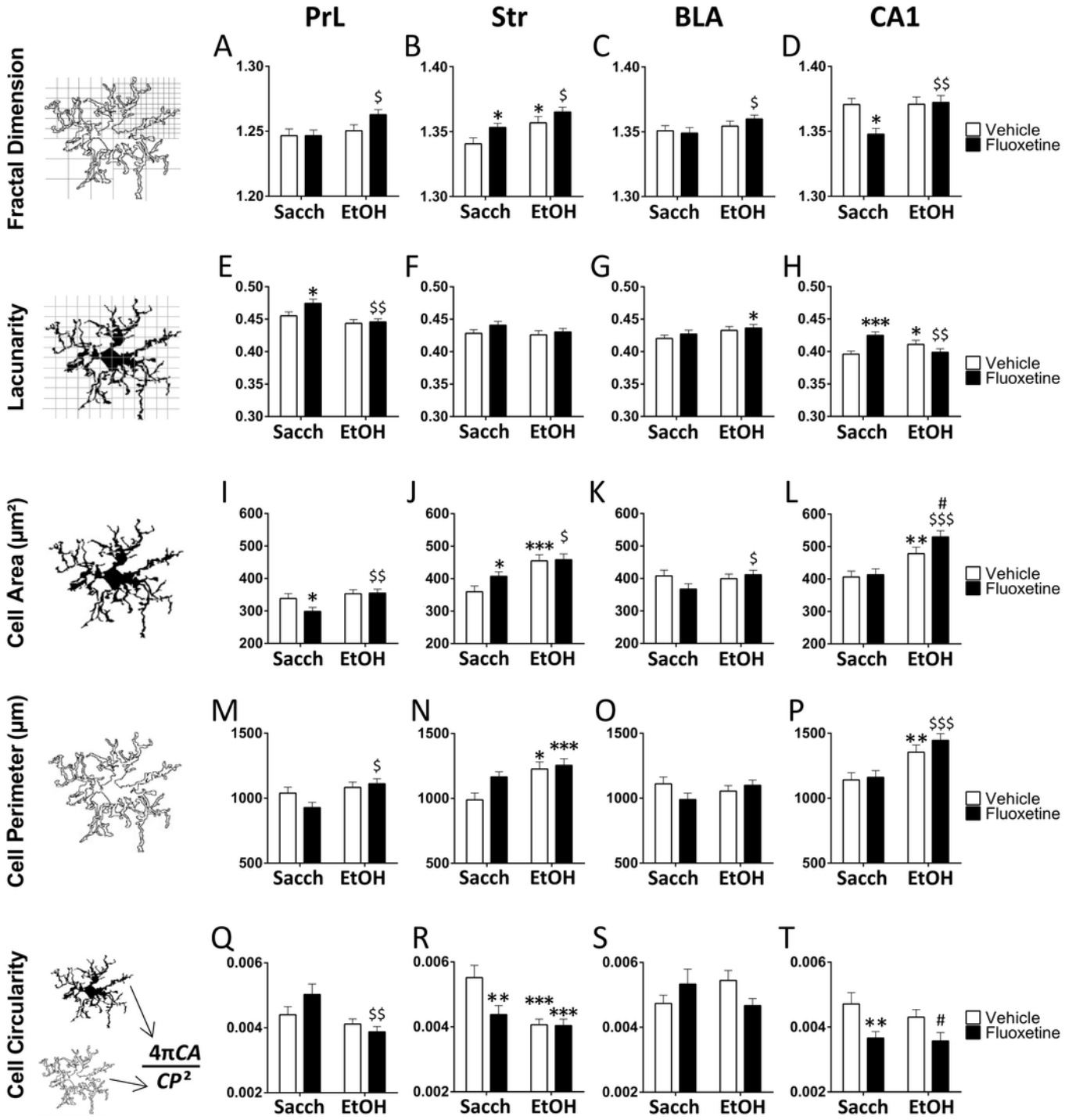

Figure 4

Effects of fluoxetine treatment cessation and ethanol drinking reinstatement on the morphometric parameters fractal dimension (A-D), lacunarity (E-H), cell area (I-L), cell perimeter (M-P), and cell circularity (Q-T) in the microglia of the prelimbic cortex (PrL), striatum (Str), basolateral amygdala (BLA), and hippocampal CA1. The histograms represent the mean + SEM (n = 50 cells per experimental group). Tukey's test: */**/***p < 0.05/0.01/0.001 vs. saccharine-vehicle group; $/

/

$p < 0.05/0.01/0.001 vs. saccharine-fluoxetine group; #p < 0.05 vs. ethanol-vehicle group.

Figure 5

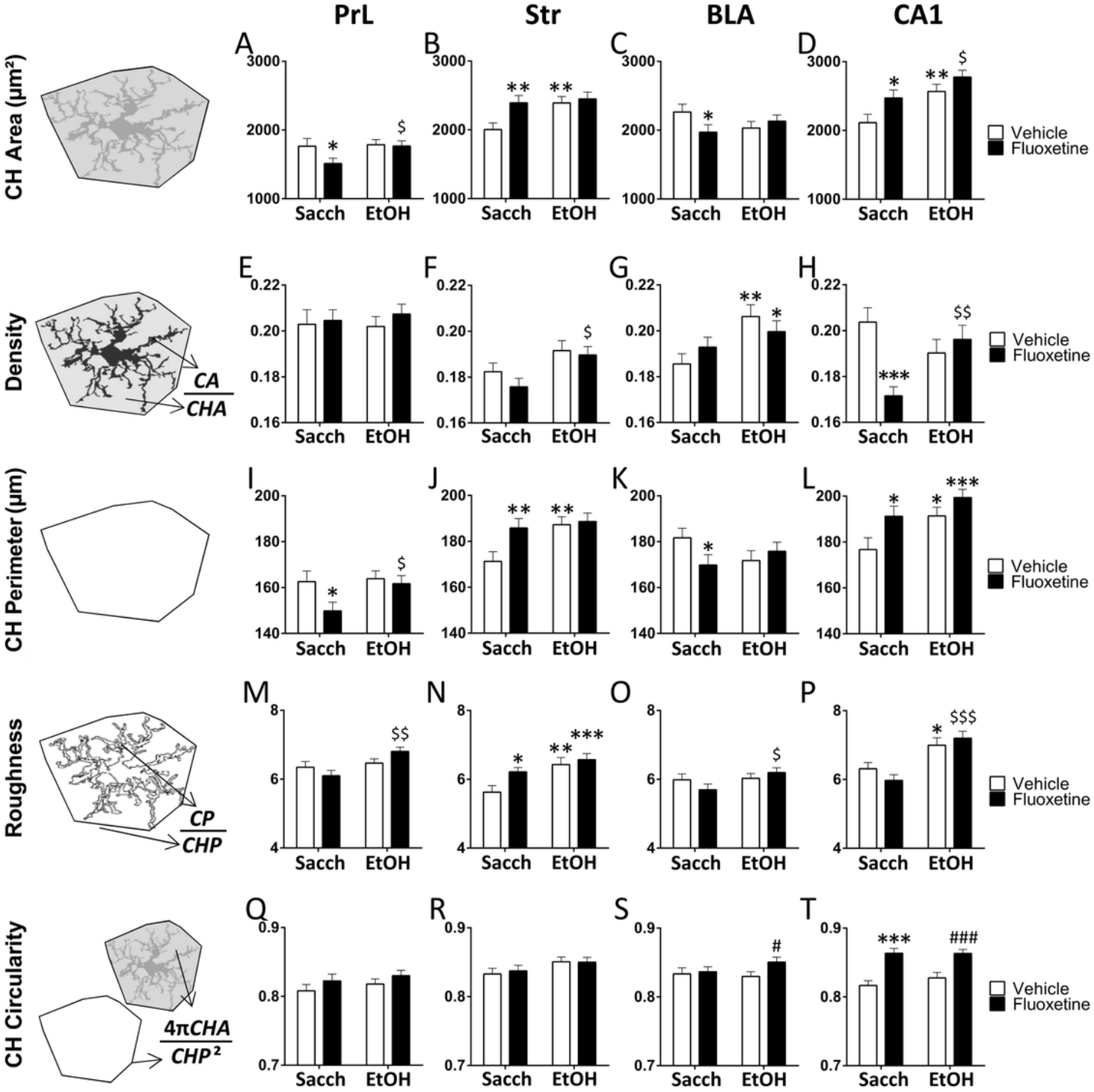

Figure 5

Effects of fluoxetine treatment cessation and ethanol drinking reinstatement on the morphometric parameters CH area (A-D), density (E-H), CH perimeter (I-L), roughness (M-P), and CH circularity (Q-T) in

the microglia of the prelimbic cortex (PrL), striatum (Str), basolateral amygdala (BLA), and hippocampal CA1. The histograms represent the mean + SEM (n = 50 cells per experimental group). Tukey's test: */**/***p < 0.05/0.01/0.001 vs. saccharine-vehicle group; $/

/

$p < 0.05/0.01/0.001 vs. saccharine-fluoxetine group; #/###p < 0.05/0.001 vs. ethanol-vehicle group.

Figure 6

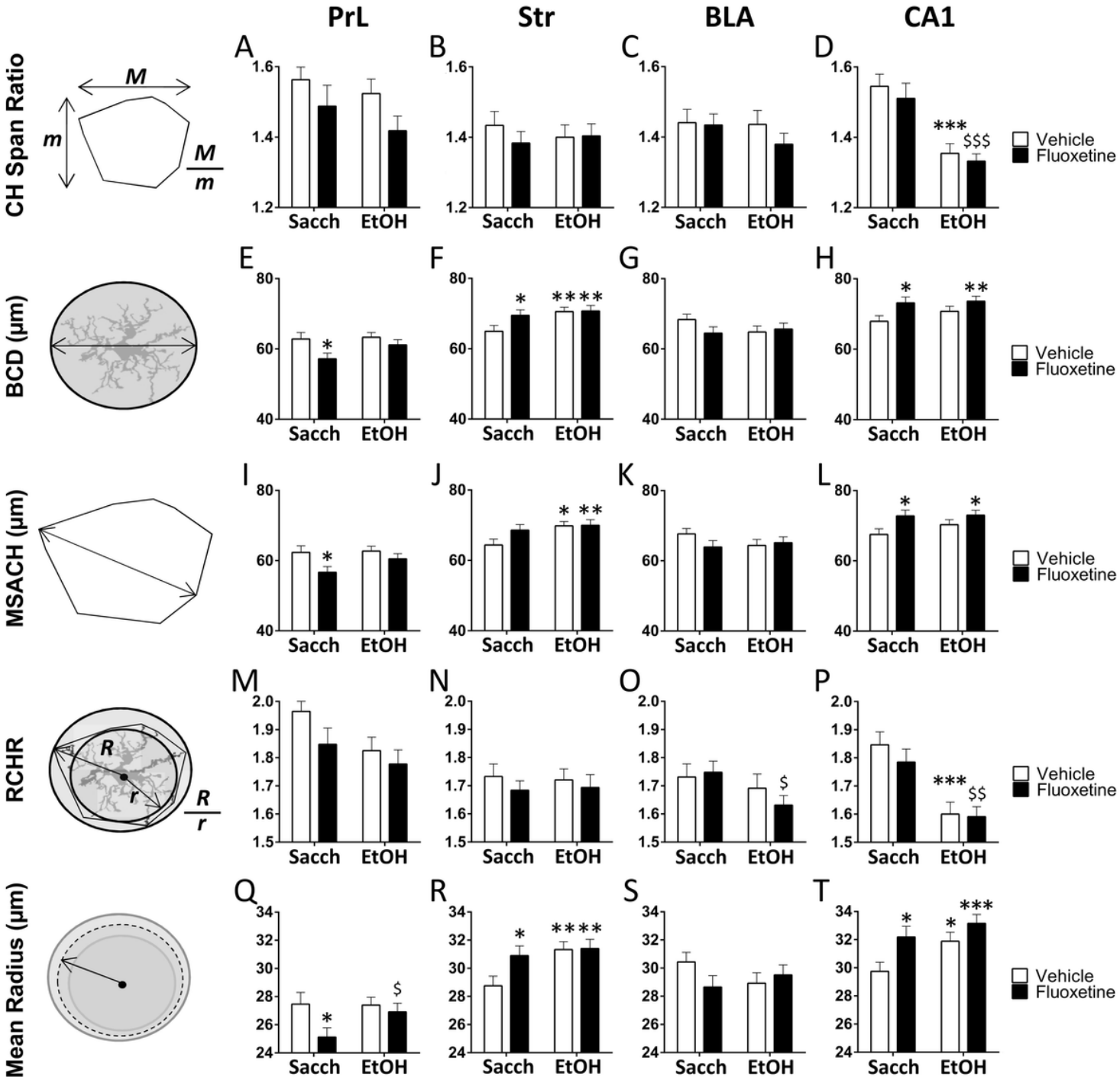

Figure 6

Effects of fluoxetine treatment cessation and ethanol drinking reinstatement on the morphometric parameters CH span ratio (A-D), BCD (E-H), MSACH (I-L), RCHR (M-P), and the mean radius (Q-T) in the microglia of the prelimbic cortex (PrL), striatum (Str), basolateral amygdala (BLA), and hippocampal CA1. The histograms represent the mean + SEM (n = 50 cells per experimental group). Tukey's test: */**/***p < 0.05/0.01/0.001 vs. saccharine-vehicle group; $/

/

$p < 0.05/0.01/0.001 vs. saccharine-fluoxetine group.

Figure 7

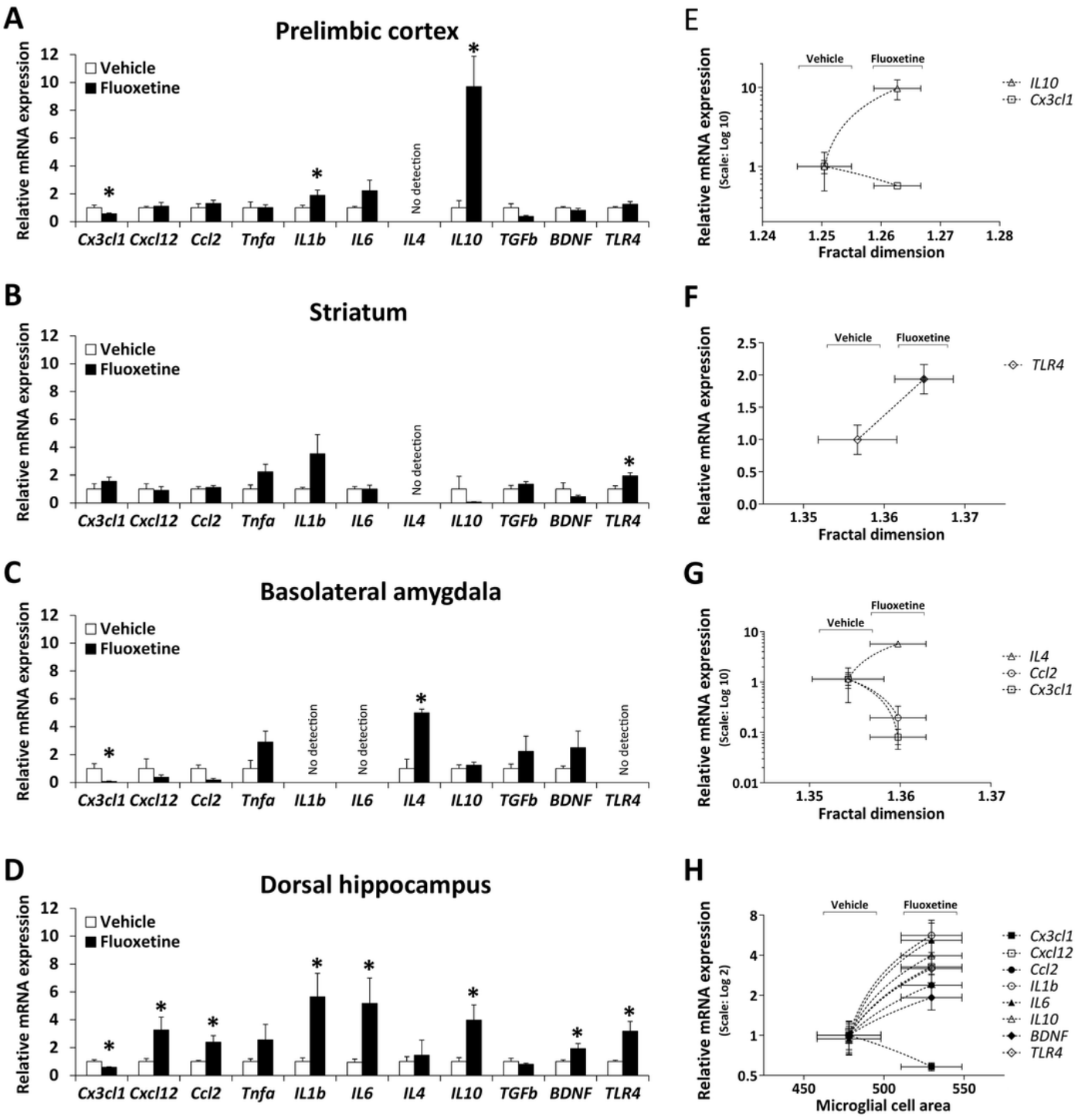

Figure 7

Effects of fluoxetine treatment cessation in rats with ethanol drinking reinstatement on the mRNA expression of inflammatory cytokines (Tnfα, IL1β, IL6, IL4, IL10, TGFβ, BDNF), chemokines (Cx3cl1, Cxcl12, Ccl2) and TLR4 in the prelimbic cortex (A), striatum (B), basolateral amygdala (C), and dorsal hippocampus (D). The histograms represent the mean + SEM (n = 7 rats per experimental group). Student's t test: *p < 0.05 vs. vehicle group. Correlation analysis between inflammatory factors and

morphometric parameters of microglia in the prelimbic cortex (E), striatum (F), basolateral amygdala (G), and dorsal hippocampus (H) when vehicle-treated rats and fluoxetine-treated rats were faced. The scatter (XY) plots represent the means ± SEM. Plotted lines between mean points indicate that fluoxetine induces significant correlative changes between the two variables represented.

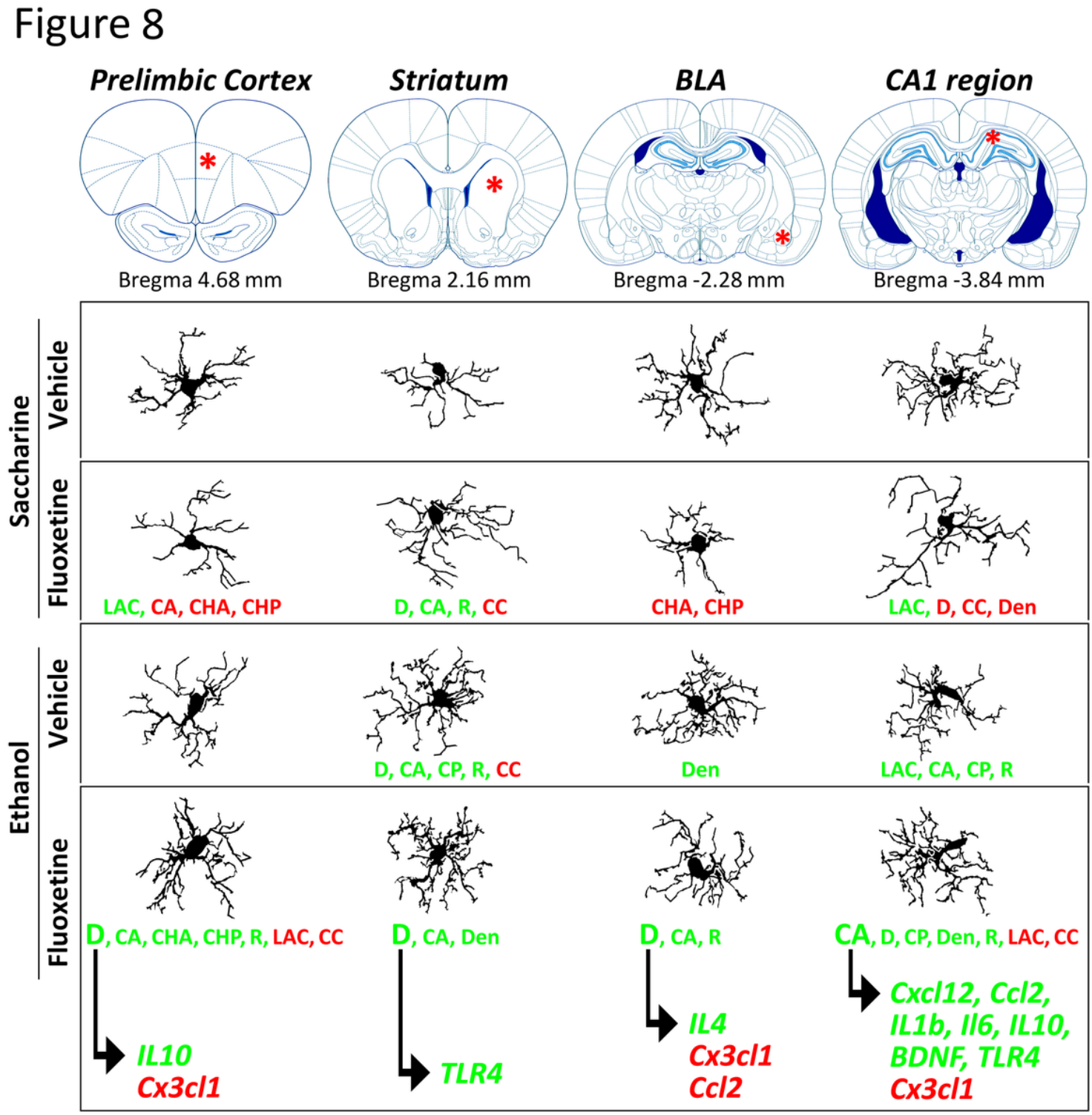

Figure 8

Schematic representation that summarize the main effects of fluoxetine treatment cessation and ethanol drinking reinstatement on microglial morphology and its association with reactive phenotype (inflammatory response) in each brain region analyzed.